17/9/76

STUDY OF DIFFUSION IN THE TWO BULB APPARATUS

MEASUREMENT OF THE SENFTLEBEN-BEENAKKER EFFECT

by

Michael Alan Yabsley B.Sc.(Hons)

A thesis presented for the degree of

Doctor of Philosophy

at the University of Adelaide

December, 1975

Department of Physical and Inorganic Chemistry

S U M M A R Y

Two different diffusion cells are described, each incorporating thermistors as the concentration detectors.

The first cell, the two bulb apparatus, was originally employed by Ney and Armistead. For the purposes of comparison, the shearing cell, based upon a design of Loschmidt, is also employed. The construction and associated theory behind each of these diffusion cells is explained at some length.

Experimental evidence is presented justifying the assumption of a direct proportionality between the difference in resistance between the two thermistors in a particular diffusion cell and the corresponding concentration difference.

Equations derived by Mason et al. are used to develop an equation describing the behaviour of a diffusing gas in a capillary at low pressures. This equation is used to describe the results obtained with the two bulb apparatus. It also offers an explanation of the anomalous behaviour observed by Van Heyningen et al. in binary systems containing helium.

With each cell, diffusion coefficients are obtained for the He/Ar and He/O_2 systems at 300K. The two bulb apparatus results require an extrapolation to yield the high pressure limiting diffusion coefficient.

Results obtained from both cells are then

compared with the predictions of the Chapman-Enskog theory. A further comparison is made with three recently formulated correlation functions.

Finally, the two bulb apparatus is utilized in an attempt to find the effect of a magnetic field upon diffusion in the Ar/O_2 system.

ACKNOWLEDGMENT

It is with much pleasure that I acknowledge the help and guidance given to me by my Supervisor, Dr. P.J. Dunlop. I would also like to thank Dr. B.J. Steel for his kind assistance with some aspects of this work.

Gratitude is due also to my associates in the Department of Physical and Inorganic Chemistry, Messrs. R.S. Murray, G.R. Staker and P.J. Carson, whom I would like to thank for their contributions during our many discussions.

The reading and criticism of the draft of this thesis by Dr. D.G. Humphreys was greatly appreciated.

Also to be acknowledged is the valuable assistance offerred me by Messrs. K.R. Shepherdson and J. Beard of the Electronics Workshop and that of Messrs. A. Bowers and J. Netting of the Mechanical Workshop.

Finally, I thank Mrs. Verna Humphreys for her diligence in typing the thesis and my Wife, Denise for the constant help she has been to me during the course of this work.

I hereby certify that this thesis contains no material which has been accepted for the award of any other Degree or Diploma in any University, and to the best of my knowledge contains no material previously published or written by any other person, except where due reference is made in the text.

TABLE OF CONTENTS

		Page
SUMMARY		i
ACKNOWLEDGMENT		iii
DECLARATION		iv
TABLE OF CONTENTS		v
LIST OF TABLES		vii
LIST OF FIGURES		ix
INTRODUCTION		1
CHAPTER I	BINARY DIFFUSION COEFFICIENTS	
	1.1 Chapman-Enskog Theory	4
	1.2 Diffusion Coefficient Equations	5
	1.3 Knudsen Diffusion	9
	1.4 Chapman-Enskog Type Treatment	12
	1.5 Pressure Gradient	14
	1.6 Diffusion Coefficient Equations at Low Pressures.	15
CHAPTER II	DIFFUSION CELLS	
	2.1 Introduction	19
	2.2 Two Bulb Apparatus	19
	2.3 Construction of the Diffusion Cell	20
	2.4 End Correction Analysis	22
	2.5 Cell Dimensions	23
	2.6 Pressure Measurements	25
	2.7 Experimental Procedure	26
	2.8 Theory of Two Bulb Apparatus.	27
	2.9 Relaxation Times	31
	2.10 Errors	32
	2.11 Shearing Cell	33
	2.12 Theory	36
	2.13 Concentration dependence of the Diffusion Coefficient	37
	2.14 Comparison between the two Cells	38

TABLE OF CONTENTS (Continued)

		Page
CHAPTER III	DIFFUSION BRIDGE ANALYSIS	
	3.1 Introduction	42
	3.2 Circuit Analysis	43
	3.3 Power Considerations	46
	3.4 Analysis	47
	3.5 Further Method of Analysis .	49
CHAPTER IV	RESULTS AND DISCUSSION	
	4.1 Diffusion Circuit Analysis .	53
	4.2 Two Bulb Apparatus Results .	57
	4.3 Shearing Cell Results	73
	4.4 Chapman-Enskog Theory	73
	4.5 Conclusion	78
CHAPTER V	EFFECT OF A MAGNETIC FIELD UPON DIFFUSION	
	5.1 Introduction	79
	5.2 Background	79
	5.3 Senftleben-Beenakker Effects.	81
	5.4 Previous Investigations . . .	83
	5.5 Present Investigation	85
	5.6 Method of Measurement	86
	5.7 Results	91
	5.8 Discussion	99
APPENDICES	. . . . .	102
REFERENCES	. . . . .	105

LIST OF TABLES

Table		*Page*
1.1	Comparison of Approximation Schemes of the Chapman-Enskog Theory	8
2.1	Dimensions of the Connecting Tubes	23
2.2	End Corrections to the Connecting Tubes	24
2.3	Bulb Volumes	25
2.4	Pycnometer Volume	25
2.5	Relaxation Times for the Two Bulb Apparatus	32
2.6	Errors in Dimension Measurements	32
4.1	Results for the system He/Ar at 300K using Circuit A. Corrections for power effects	54
4.2	Diffusion Coefficients for the system He/Ar at 300K as a function of $(Pr)^{-1}$	58
4.3	Diffusion Coefficients for the system He/O_2 at 300K as a function of $(Pr)^{-1}$	61
4.4	Comparison of Parameters obtained from eqn. (1.19) and those of a Least-Squares Analysis of the data	64
4.5	Two Bulb Apparatus Results for the Concentration Dependence of the Diffusion Coefficient for the system He/Ar at 300K	66

LIST OF TABLES (Continued)

Table		*Page*
4.6	Two Bulb Apparatus Results for the Concentration Dependence of the Diffusion Coefficient for the system He/O_2 at 300K	67
4.7	Shearing Cell Results for the Concentration Dependence of the Diffusion Coefficient for the system He/Ar at 300K	69
4.8	Shearing Cell Results for the Concentration Dependence of the Diffusion Coefficient for the system He/O_2 at 300K	71
4.9	Least-square parameters of eqn. (4.1) for the systems He/Ar and He/O_2	74
4.10	Predicted Diffusion Coefficients for the systems He/Ar and He/O_2 at 300K using Kihara's second approximation . .	75
4.11	Comparison of Experimental and Predicted Values of $(P\mathcal{D}_{12})_{x_2=1} / (P\mathcal{D}_{12})_{x_2=0}$ . . .	76
4.12	Comparison of Experimental Results with three Correlation Functions	77
5.1	Results for the effect of a Magnetic Field upon Binary Diffusion for the System Ar/O_2	92
5.2	Summary of Results presented in Table (5.1)	98

LIST OF FIGURES

Figure		*Page*
1.1	Typical plot of (PD_{12}) as a function of $(Pr)^{-1}$ for the system He/O_2 at 300K	18
2.1	The Two Bulb Apparatus	21
2.2	The Shearing Cell	34
3.1	The Wheatstone Bridge Circuit	44
3.2	Plot of Apparent Thermal Conductivity as a Function of Concentration for the system He/Ar	51
4.1	Comparison between Diffusion Coefficient Results obtained using Circuit A and Circuit B	56
4.2	(PD_{12}) as a function of $(Pr)^{-1}$ for the system He/Ar at 300K	60
4.3	(PD_{12}) as a function of $(Pr)^{-1}$ for the system He/O_2 at 300K	63
4.4	Concentration Dependence of the Diffusion Coefficient for the system He/Ar at 300K	70
4.5	Concentration Dependence of the Diffusion Coefficient for the system He/O_2 at 300K	72
5.1	Concentration as a Function of Time showing Division into Segments	88

INTRODUCTION

In recent years a number of papers[1-8] have been published dealing with binary diffusion coefficients as measured by the method involving thermistors as concentration detectors. The results of van Heijningen et al.[1,2] are noteworthy in that they present diffusion data as a function of concentration over a wide range of temperatures.

It would appear, however, that because of their experimental reproducibility of 1 - 2% some finer details of the Chapman-Enskog theory[9] have been overlooked.

In the first chapter of this thesis a brief description will be given of the Chapman-Enskog theory of diffusion. However, these results are restricted to the dilute gas region where gas-wall interactions are negligible.

Employing equations derived by Mason et al.[10] to describe flow in porous media, capillary diffusion being a particular example of this flow type, expressions will be derived describing the behaviour of a diffusing gas in a capillary.

In the second chapter, two different types of cell are described. The first is a two bulb apparatus, based upon a design of Ney and Armistead,[11] which is constructed to operate at low pressures. The second cell type is a shearing cell based upon the design of Loschmidt.[12] Both cells incorporate two thermistors for the measurement

of the concentration changes. The basic construction and underlying theory of both cells is explained.

In the subsequent chapter, the problem of the proportionality between the difference in resistance between the two thermistors and the corresponding concentration difference is considered. An expression is derived showing a direct proportionality, under normal experimental conditions, in one of the circuits analysed. Results are also given that confirm the method of measuring concentration differences in this work as being legitimate.

In Chapter IV the experimental results are presented showing the concentration dependence of two systems, He/Ar and He/O_2, using the two different diffusion cells described.

The results for the two bulb apparatus require a further interpretation since gas-wall collisions contribute to the diffusion coefficient. Equations derived in Chapter I are used to explain these results.

Further analysis of these equations provides an explanation for the anomalous results obtained by van Heijningen et al.[2] for concentration dependence studies of systems containing helium.

Finally, results obtained using the two diffusion cells are compared. The theoretical concentration dependence of the two binary systems is calculated using the results of the Chapman-Enskog theory. A comparison is made between the experimental results and the predictions of this theory.

The last chapter is a study of the magnetic field

effect, the so called "Senftleben-Beenakker" effect, upon diffusion. Magnetic fields change the transport processes of most polyatomic molecules. However, in the case of diffusion,[13,14] no such effect has been observed.

The two bulb apparatus has been used in this work to study the postulated effect. The procedure and results obtained from the Ar/O_2 system will be detailed in the concluding chapter.

CHAPTER I

BINARY DIFFUSION COEFFICIENTS

1.1 Chapman-Enskog Theory

Modern kinetic theory has developed from Maxwell's statistical description of gas behaviour. Following Maxwell's work, Boltzmann formulated an integro-differential equation describing the velocity distribution function for molecules in space and time. The solution of Boltzmann's equation yields a full description of transport processes in dilute gases.

A solution of Boltzmann's equation[9] was independently and simultaneously formalised by Chapman and Enskog, as implied in the name. The solution contains the following assumptions:

(i) *Only binary collisions occur.*

This assumption is inherent in the derivation of Boltzmann's equation and, therefore, restricts the application of the solution to dilute gases.

(ii) *Molecules possess small mean free paths.*

At moderate pressures, collisions with confining walls are insignificant. This treatment does not account for gas-wall collisions, which become important at lower pressures. This point will be considered in greater detail in section (1.3).

(iii) *Small perturbations.*

All transport processes arise out of deviations from an equilibrium situation. It must be assumed that these perturbations are small so that the molecular fluxes have linear gradients.

(iv) *Elastic Collisions.*

Molecules are considered to be monatomic. However, as diffusion is not greatly dependent upon the presence of internal degrees of freedom, the theory may be considered applicable to simple polyatomic molecules.

The Chapman-Enskog solution of Boltzmann's equation describes the diffusion coefficient as a single unknown in an infinite set of equations which cannot be solved exactly. The solution involves a method of successive approximations. Two such procedures commonly used are the method of Chapman and Cowling and that of Kihara.

Kihara's method is somewhat simpler and convergence occurs more rapidly than in the treatment of Chapman and Cowling. However, it has the disadvantage of being difficult to generalise beyond the second approximation. Fortunately, the convergence of both of these procedures is very rapid. (See section (1.2)).

1.2 Diffusion Coefficient Equations

The first approximation to the diffusion

coefficient is identical for both schemes and can be written thus:

$$(\mathscr{D}_{12})_1 = \frac{3}{8\sqrt{\pi}} \left(\frac{k^3T^3}{2\mu_{12}}\right)^{\frac{1}{2}} \frac{1}{P\sigma_{12}^2\Omega_{12}^{(1,1)*}} \qquad (1.1)$$

where $\mu_{12} = (m_1m_2)/(m_1 + m_2)$ is the reduced mass, T the temperature, k Boltzmann's constant, P the pressure, σ_{12} the distance between the molecules when the interaction energy is zero and $\Omega_{12}^{(1,1)*}$ the reduced diffusion collision integral being a function of the reduced temperature T^* ($T^* = kT/\varepsilon$ where ε is the depth of the potential energy well).

Collision integrals represent an effective cross section for the scattering process and, as such, depend upon the choice of the intermolecular potential function.

The higher approximations of both methods may be written as:

$$(\mathscr{D}_{12})_M = (\mathscr{D}_{12})_1 \, f_D^{(M)} \qquad (1.2)$$

where $f_D^{(M)}$ accounts for higher approximations.

The Chapman-Cowling second approximation may be written as:

$$(\mathscr{D}_{12})_2 = (\mathscr{D}_{12})_1(1/(1-\Delta_{12})) \qquad (1.3)$$

whereas the relevant Kihara expression takes the form:

$$(\mathscr{D}_{12})_2 = (\mathscr{D}_{12})_1(1+\Delta_{12}) \qquad (1.4)$$

The coefficient, Δ_{12}, is defined as:

$$\Delta_{12} = \frac{(6C_{12}^{*}-5)^2}{10} \left(\frac{x_1^2P_1+x_2^2P_2+x_1x_2P_{12}}{x_1^2Q_1+x_2^2Q_2+x_1x_2Q_{12}}\right) \qquad (1.5)$$

where x_1 and x_2 are the mole fractions of the light and

heavy gas respectively, C_{12}^{*} is a ratio of collision integrals and the P's and Q's are complicated expressions involving various collision integrals as well as molecular weights. These expressions differ slightly for the two methods of approximation. (Appendix I)

Most of the composition dependence of the diffusion coefficient is contained in eqn. (1.5). Expressions for the higher approximations to the Chapman-Cowling method are extremely complicated and appropriate equations may be found in refs. (15) and (16).

At this stage it is worthwhile to compare the two schemes for varying orders of approximation.

In Table (1.1) below, the ratio $(\mathcal{D}_{12})_4/(\mathcal{D}_{12})_1$ is given for the Chapman-Cowling method and these results are compared with the ratio $(\mathcal{D}_{12})_2/(\mathcal{D}_{12})_1$ for Kihara's method. The He/Ar system at 300K is used in this example. Like and unlike parameters were obtained from ref. (2) and collision integrals for the Lennard-Jones (12,6) potential function from refs. (17) and (18).

Table (1.1)

Comparison of Approximation Schemes of the Chapman-Enskog Theory

x_2	Chapman-Cowling $(\mathscr{D}_{12})_4/(\mathscr{D}_{12})_1$	Kihara $(\mathscr{D}_{12})_2/(\mathscr{D}_{12})_1$
0	1.0002	1.000
0.1	1.0079	1.0079
0.2	1.0137	1.0144
0.3	1.0184	1.0195
0.4	1.0222	1.0236
0.5	1.0253	1.0268
0.6	1.0279	1.0293
0.7	1.0302	1.0313
0.8	1.0321	1.0328
0.9	1.0338	1.0340
1.0	1.0353	1.0350

Such calculations indicate that convergence of both procedures is complete after four steps and that the Kihara second approximation is sufficient to describe the entire concentration dependence of the diffusion coefficient.

In Chapter IV experimental results will be compared with Kihara's second approximation to the Chapman-Enskog theory.

1.3 Knudsen Diffusion

A basic assumption in the Chapman-Enskog solution to Boltzmann's equation is that the molecules have small mean free paths. If gas-wall collisions do become important, their effect is not predicted by the Chapman-Enskog solution.

In one of the diffusion cells employed in this work, gas-wall collisions are important and their effect must be taken into consideration.

In the following sections two treatments of the problem will be considered. The first, a momentum transfer argument given by Pollard and Present[19] and then a complete Chapman-Enskog type treatment of the problem.

Elementary treatments.

Diffusion through a capillary is considered for all following discussions. The mean free path, ℓ, may be defined as:

$$\ell = (\sqrt{2}\ \pi\ n\ \sigma^2)^{-1} \qquad (1.6)$$

n being the number density and σ the distance of closest approach.

At very low pressures, the mean free path becomes large in comparison to the capillary diameter, and consequently, the diffusion coefficient, D_{iK}, is defined by the capillary dimensions, namely:

$$D_{iK} = 2/3\bar{v}_i r \qquad i = (1,2) \qquad (1.7)$$

where r is the capillary radius and $\bar{v}_i$ the mean Maxwell-

ian velocity defined thus:

$$\bar{v}_i = \left(\frac{8RT}{\pi M_i}\right)^{\frac{1}{2}} \qquad i = 1,2 \qquad (1.8)$$

The subscript, K, refers to the low pressure, or Knudsen diffusion coefficient and the M_i are the molecular weights of the gases.

At these pressures, the gases will diffuse independently. At higher pressures, where intermolecular collisions predominate, the normal Chapman-Enskog diffusion coefficient, $\mathcal{D}_{12}$ defined in eqn. (1.2) prevails.

In the region between "normal" and Knudsen diffusion, the so called "transition region", the behaviour lies somewhere between these limits.

In the treatise of Pollard and Present,[19] equations relating the effective self diffusion coefficient to the capillary radius and mean free path were derived. These equations are:

$$(D_1)_{eff} = D_{1K}\left(1 - \left(1.2264 + 3/4\ln\left(\frac{\ell}{2\gamma r}\right)\right)\frac{r}{\ell} + \ldots\right) \qquad \ell > r \qquad (1.9a)$$

$$(D_1)_{eff} = D_{11}\left(1 - \frac{3}{8}\frac{\ell}{r}\right) \qquad \ell < r \qquad (1.9b)$$

$$D_{11} = \frac{1}{3}\bar{v}_1\ell$$

where γ is Euler's constant, $(D_1)_{eff}$ the effective self diffusion coefficient and D_{11} is the mean free path expression for the self diffusion coefficient.

Equation (1.9a) reduces to the Knudsen diffusion coefficient at very low pressures and at relatively small mean free paths a linear dependence of the self diffusion

coefficient upon $(Pr)^{-1}$ is predicted by eqn. (1.9b). (The mean free path is inversely proportional to pressure.)

This treatment is successful in deriving equations that predict the diffusion behaviour at the two extremes of pressure, but it does not provide any description of diffusion in the transition region.

The following expression, in the same form as eqn. (1.9b), was rationalised by Van Heijningen et al.[1,2] for binary diffusion:

$$(PD_{12}) = (P\mathscr{D}_{12})\left(1 - \frac{C_1 \ell}{r}\right) \qquad (1.10)$$

where C_1 is a constant and D_{12} is the effective binary diffusion coefficient taking into account gas-wall collisions.

Substituting eqn. (1.6) into this expression gives:

$$(PD_{12}) = (P\mathscr{D}_{12})(1 - \frac{C_2}{Pr}) \qquad (1.11)$$

C_2 being a redefined constant.

This equation predicts that the diffusion coefficient will be a linear function of $(Pr)^{-1}$. However, the concentration dependence of the mean free path must be considered. This takes the form:[20]

$$\ell_i = (\sqrt{2}\pi n_i \sigma_{ii}^2 + n_j \sigma_{ij}^2 \left(1 + \frac{M_i}{M_j}\right)^{\frac{1}{2}})^{-1} \qquad (1.12)$$

$$i,j = 1,2 \quad i \neq j$$

where the subscripts ii and ij refer to the type of interaction.

A concentration averaged mean free path may be

written as:

$$\ell_{av} = x_1\ell_1 + x_2\ell_2 \qquad (1.13)$$

This average has been employed in other applications.[21,22] For binary gas mixtures, ℓ_{av} should replace ℓ in eqn. (1.10). As in eqn. (1.9b), this expression predicts a linear dependence of the diffusion coefficient upon $(Pr)^{-1}$. Once again there is no indication of how the diffusion coefficient behaves in the transition region and at what values of $(Pr)^{-1}$ do such effects become important.

In the following section a Chapman-Enskog type treatment of the problem will be given which provides a full description of a diffusing gas in a capillary.

1.4 Chapman-Enskog Type Treatment:

Equation (1.11) was deduced from elementary arguments and, therefore, suffers from the limitations inherent in any simple treatment.

In a series of papers Mason[23-26] et al. considered the effects of composition, pressure and temperature gradients upon the diffusion process in porous media. These results were subsequently improved upon in a further publication.[10]

The porous media is visualised as a hypothetical array of giant dust particles which are held stationary in space. Flow through such a medium involves diffusive, viscous and geometrical considerations. By assigning appropriate geometrical constants, equations derived from such a treatment are applicable to diffusion in a capillary.

Zhdanov et al.,[27] using an expansion of the Maxwell distribution function by Grad's 13-moment method, derived flux equations in terms of pressure, composition and temperature gradients.

Using these equations as a starting point, Mason et al.[10] derived expressions for the individual fluxes of the gases by employing the proposed "dusty gas" model. A specific example of the results is diffusion along a capillary at constant temperature and no net flow.

The derived equations are as follows:

$$J_1 = -(D_{1E})(dn_1/dz) + x_1\delta_1 J$$

$$-x_1(1-\delta_1)(r^2/8\eta kT)P(dP/dz) \qquad (1.14a)$$

$$J - \beta_1 J_1 = -(D_{2K}/kT)\left[1 + \left\{\frac{x_1}{D_{1K}} + \frac{x_2}{D_{2K}}\right\}\frac{r^2 P}{8\eta}\right]\frac{dP}{dz} \qquad (1.14b)$$

where $(D_{1E})^{-1} = (\mathcal{D}_{12})^{-1} + (D_{1K})^{-1}$

$$\delta_1 = ((D_{1E})/(\mathcal{D}_{12}))$$

$$\beta_1 = 1 - (D_{2K}/D_{1K}) = 1 - (M_1/M_2)^{\frac{1}{2}}$$

J_1 being the flux of species 1, J the total flux, (D_{1E}) an effective binary diffusion coefficient and (dP/dz) the pressure gradient established along the capillary. For a closed system, the total flux, J, equals zero. Expressions for the second component are found by interchange of subscripts.

A small pressure gradient must exist since the individual fluxes of the gases differ. This pressure gradient then counteracts the effect of the dissimilar fluxes and establishes a quasi-steady state.

1.5 Pressure Gradient:

An expression for the pressure gradient along a capillary may be obtained as follows:

Eliminating J_1 from eqn. (1.14) yields, after some manipulation, the following differential equation:

$$(dP/dx_1) = -P\beta_1\left[(1-\beta_1) + \left(\frac{3}{16\bar{v}_1\eta} + \frac{2\bar{v}_2}{3(P\mathcal{D}_{12})}\right) Pr + \frac{(1-x_1\beta_1)}{8\eta(P\mathcal{D}_{12})}(Pr)^2\right]^{-1} \quad (1.15)$$

If the first two terms of this equation are set to zero, the resulting expression may be integrated to yield:

$$\Delta P = \frac{8\bar{\eta}\mathcal{D}_{12}}{r^2} \ln\left(\frac{1-\beta_1 x_1(L)}{1-\beta_1 x_1(0)}\right) \quad (1.16)$$

where $\bar{\eta}$ is an averaged viscosity and $x_1(0)$ and $x_1(L)$ refer to the mole fraction of gas at the lower and upper ends of the capillary, respectively.

This expression was first derived by Kramers and Kistemaker[28] in 1943 in relation to the pressure gradient established during diffusion in very fine capillaries. Little interest was shown in the subject until 17 years later when McCarty and Mason[29] rediscovered the effect, which became the subject of considerable theoretical and experimental investigations.[30-33]

Equation (1.15) is applicable at all pressures. Of the terms enclosed in the brackets, the first is important at extremely low pressures where the predominant collisions are of the gas-wall type, the second term at intermediate pressures and the third term at higher pressures.

Integration of eqn. (1.15) is difficult, but if the differential approximations of $\Delta P \simeq dP$ and $\Delta x_1 \simeq dx_1$ are made, and the mean values of x_1, x_2, η, and P taken, then the resulting equation becomes the Kramers-Kistemaker effect at all pressures.

1.6 Diffusion Coefficient Equations at Low Pressures

If a steady state is assumed and the diffusion coefficient is considered to be independent of composition, then eqn. (1.14a) may be used to derive an expression relating the experimental diffusion coefficient to the Chapman-Enskog diffusion coefficient.

Equation (1.14a) may be written in the form:

$$J_1 = -nD_{12}(dx_1/dz) \qquad (1.17)$$

where $D_{12} = (D_{1E} - x_1(1 - \delta_1)(r^2/8\eta)(dP/dx_1)$

This equation is in the form of Fick's first law, the quantity, D_{12}, being an *apparent* diffusion coefficient containing contributions from both Knudsen and viscous flows. It is this quantity that is measured in this type of cell.

Equations (1.14b) and (1.17) may be integrated, along the connecting tube, by making appropriate differential approximations, once again substituting the mean

values for x_1, x_2, η and P. Combining the two resulting equations and substituting for the pressure gradient, ΔP, derived in section (1.5), yields, after some manipulations:

$$(PD_{12})=(P\mathcal{D}_{12})(1+A(Pr)^{-1})(1+(A+B)(Pr)^{-1}+C(Pr)^{-2})^{-1} \tag{1.18a}$$

where

$$A = (16/3)\bar{v}_2\eta b \tag{1.18b}$$

$$B = (P\mathcal{D}_{12})b/(2/3\bar{v}_1) \tag{1.18c}$$

$$C = 8\eta b(P\mathcal{D}_{12})(1-\beta_1) \tag{1.18d}$$

$$b = (1-x_1\beta_1)^{-1} \tag{1.18e}$$

This equation provides a full description of a diffusing gas in a capillary of radius, r, and at a total pressure, P. Appropriate geometrical constants given by Mason et al.[10] have been substituted into the equation above.

One of these constants does require some discussion. This is the so called slip factor which is introduced as a constant in eqn. (1.7). This factor takes the value of 0.59 according to Maxwell's theory of slip, 0.81 according to Knudsen's experiments and the calculations of Mason et al. reveal a value of 0.9. The limiting value of this coefficient is one. It will be seen in Chapter IV that the experimental results of this work are best reproduced by eqn. (1.18) if a value of one is employed.

A typical plot of this function is presented in

fig. (1.1) for the system He/O_2 at 300K. At low values of $(Pr)^{-1}$ the graph is linear with deviations occurring at higher values of the abscissa.

For low values of $(Pr)^{-1}$ eqn. (1.18) may be approximated to:

$$(PD_{12}) = (P\mathcal{D}_{12})(1-B(Pr)^{-1}) \qquad (1.19)$$

the limiting slope being given by $(-B(P\mathcal{D}_{12}))$. Calculations show that deviations of eqn. (1.18) from this limiting function amounts to 0.2% at $(Pr)^{-1}$ equal to 3500 $(atm.cm)^{-1}$ increasing to approximately 1% at $(Pr)^{-1}$ equal to 6800 $(atm.cm)^{-1}$. For the apparatus used in this work, (Chapter II) eqn. (1.19) suffices.

Equation (1.19) may be rewritten in the form:

$$(P\mathcal{D}_{12}) = (PD_{12})(1+B'(PD_{12})(Pr)^{-1} + 2(B'(PD_{12})(Pr)^{-1})^2+....) \qquad (1.20)$$

where $B' = b/(2/3\bar{v}_1)$

providing a direct method of calculating the Chapman-Enskog diffusion coefficient for low values of $(Pr)^{-1}$.

Equation (1.18) should be used as a fitting function, the only unknown being $(P\mathcal{D}_{12})$. By minimizing the residuals between experimental and predicted data, the curve of best fit may be obtained.

Comparison with experimental results will be given in Chapter IV.

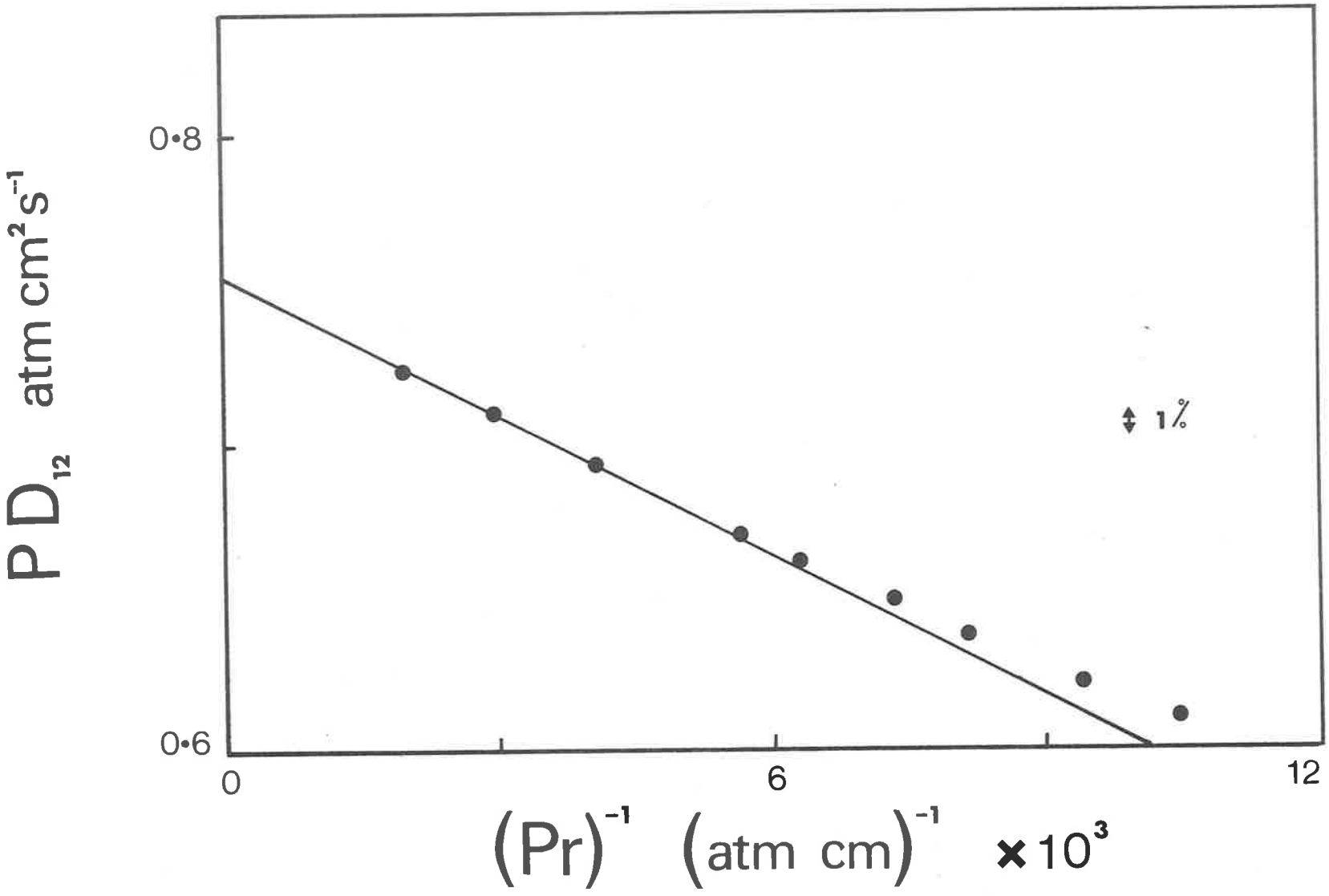

1.1 Typical plot of (PD_{12}) as a function of $(Pr)^{-1}$ for the system He/O_2 at 300K.

CHAPTER II

DIFFUSION CELLS

2.1 Introduction

Two types of diffusion cell will be considered in this chapter. The first, a two bulb apparatus, was developed by Ney and Armistead[11] to study the self diffusion of UF_6. For comparison, a shearing cell based upon the design of Loschmidt[12] is utilized. Relevant approximations made in the theory of both cells will be treated. Effects due to the non-ideality of the gases used will also be considered.

2.2 Two Bulb Apparatus

The following assumptions were made by Ney and Armistead:

(i) The volume of the connecting tube is negligible when compared to the volume of each bulb.

(ii) A quasi-stationary state exists implying that the flux of a component is constant along the connecting tube and, therefore, a linear variation in composition exists.

(iii) The composition gradient lies entirely along the length of the connecting tube, plus a certain distance beyond each end. In other words, it is assumed that an appropriate end correction made to the tube length adequately defines the extent

of the concentration gradient. The end correction is analagous to the theory appertaining to sound.[34]

Intelligent design of the apparatus may minimize errors resulting from the above assumptions. The significance of these assumptions will be discussed later.

2.3 Construction of the Diffusion Cell

Reference may be made to the accompanying diagram. (fig. 2.1)

The bulbs were constructed from type 316 stainless steel, while the connecting tubes were precision-bore brass rods which were fitted to the bulbs using swagelok fittings. All taps shown were Nupro bellows valves. (Crawford Fitting Co., Cleveland, Ohio)

As experiments were performed at pressures of several torr, it was necessary to take extra precautions against leakage. To this end, all taps and fittings were argon welded. The leak rate of the cell was better than 4×10^{-6} torr/min.

Stainless steel flexible tubing was employed to connect the cell to the gas cylinders and vacuum system.

An Edwards diffusion pump, incorporating a rotary pump, was used to obtain pressures of 2×10^{-6} torr after several hours of operation.

Pressure measurements were made using a manometer containing "degassed" silicone oil. (Dow Corning 704) Special attention was needed to ensure complete "degassing". This was achieved with the aid of a small magnetically operated stirring device.

The cell was mounted in a large waterbath and

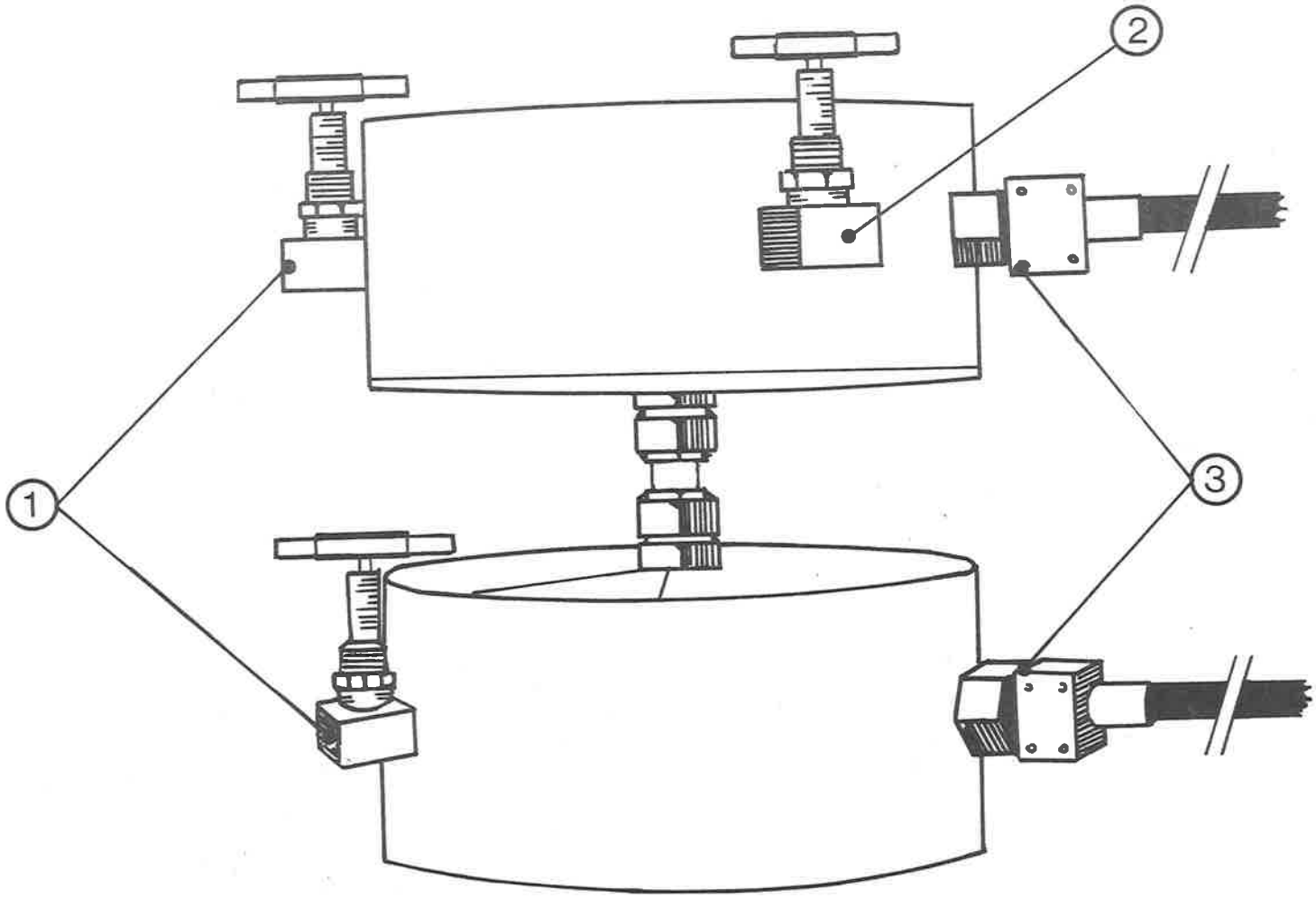

Fig. 2.1 The Two Bulb Apparatus.

1. To Vacuum and Gas Cylinders
2. To Oil Manometer
3. Thermistors

vertically aligned with a spirit level. Temperature was maintained at 300K and controlled to within ± 0.001K by means of an on-off type mercury-toluene regulator.[35]

Concentration changes were monitored with two Fenwal type G 112 P thermistors, one in each bulb. Seals between the cell and thermistors were made vacuum tight using O-rings. Electrical connections to the Wheatstone bridge were made with shielded two-core cable. Full details of the thermistors and of the bridge circuit used will be given in Chapter III.

2.4 End Correction Analysis

It was found necessary in construction to advance the connecting tube into the cell, resulting in a well defined flange, namely the annulus at the end of the tube.

As mentioned earlier, the concentration gradient does not terminate at the end of the tube but continues into the bulbs. For an infinite flange,[34] the end correction is found to be 0.82r (r being the tube radius), whereas when no flange[34,36] exists, the correction is 0.58r.

In practice, the flanges at the ends of the connecting tube lie between these two extremes and, therefore, the end correction must fall between the limits aforementioned.

Paul Wirz[37] investigated the problem of end correction variation with flange width and constructed a series of tubes of different diameters and lengths. He assumed that the correction behaved exponentially and fitted the

data to the equation:

$$\alpha = 0.60 + 0.22 \exp(-kr/w) \qquad (2.1)$$

(α being the end correction, k a constant and w the flange width)

Wirz found that the value of the constant, k, was limited by $0.129 < k < 0.136$. Applying the method of least-squares[38] to the data in this paper and weighting each point according to the quoted error gives:

$$\alpha = 0.596 + 0.219 \exp(-0.125r/w) \qquad (2.2)$$

The value of k and the limits of 0.6 and 0.82 used by Wirz are in excellent agreement with the parameters from the "least-square fit".

2.5 Cell Dimensions

Set out below are the dimensions of the two connecting tubes used. The error in the diameter of each tube was less than ± 0.00015 cm and the lengths, L, were measured within an accuracy of ± 0.002 cm.

Table (2.1)

Dimensions of the Connecting Tubes

	L (cm)	error (%)	radius (cm)	error (%)
1	18.052	± 0.01	0.2763	± 0.05
2	68.186	± 0.003	0.5353	± 0.03

To determine the correction, one must know the external diameter of the connecting tube. In the table following, the relevant dimensions and the corresponding end corrections calculated from eqn. (2.2) are given. *Note* that $2\alpha r$ is added to the measured length providing correction for each end of the tube.

$$\text{Thus } L_{eff} = L + 2\alpha r \qquad (2.3)$$

Table (2.2)

End Corrections to the Connecting Tubes

	ext. diam. (cm)	r/W	end correction	L_{eff} (cm)
1	2.22	0.332	0.81	18.500
2	2.22	0.934	0.79	69.032

The volumes of the bulbs were determined by the addition of known masses of water until the bulbs were filled. Appropriate buoyancy corrections were made and the measurements performed in duplicate.

Results are summarized in the following table:

Table (2.3)

Bulb Volumes

Upper Bulb		Lower Bulb	
Volume (cm^3)	Average	Volume (cm^3)	Average
5880.0	5879.4	5824.3	5824.2
5878.9		5824.1	

Volumes were reproducible to within 1.5 cm^3, amounting to an uncertainty of ±0.03%.

2.6 Pressure Measurements

An oil manometer was used to measure the pressure of gas in the cell. An accurate determination of the density was made using the method of pycnometry.[39]

Firstly, the volume of the pycnometer was obtained. This is given below:

Table (2.4)

Pycnometer Volume

Volume (cm^3)	Average
33.2762	33.2763
33.2764	

Due allowance was again made for buoyancy. One of the problems in determining the density of silicone oil is the short time required to completely saturate the oil with air. The density was measured without degassing and this was found to be 1.0601 g/cm^3. After several hours of evacuating, vigorous stirring and filling the pycnometer as rapidly as possible, the density was 1.0600 g/cm^3.

There appeared, therefore, to be no significant difference between the two determinations, although the amount of air absorbed in the second case remained indeterminate.

The local gravitational acceleration[40] was 979.724 cm^2/s. The standard value being 980.665 cm^2/s, all pressure measurements were reduced accordingly.

Use was made of a cathetometer to measure the head of silicone oil in the manometer. Care was taken at all times to ensure that the cathetometer was vertically mounted using a spirit level in two perpendicular planes. Thus aligned, the telescope was adjusted to give the same reading in each arm of the manometer when both sides were equally evacuated.

2.7 Experimental Procedure

Experiments were performed in the following manner.

The first gas was admitted to the cell and allowed to establish temperature equilibrium. Pressure measurements were recorded. A second gas was allowed to fill the manifold of the apparatus at a greater pressure than within the cell and achieve temperature equilibrium. The

second gas was then admitted to the appropriate bulb, depending upon relative densities of the gases, so that gravitational effects could be ignored. The oil manometer was isolated from the upper bulb, thus precisely defining the bulb volume.

At the completion of the experiment, this tap was reopened and the final pressure recorded. Any errors incurred, due to slight pressure differences between the cell and manometer, were negligible. Mole fractions were calculated from partial pressures.

2.8 Theory of Two Bulb Apparatus

Diffusional flow in a tube may be described by Fick's first law:

$$J = -\mathcal{D}_{12} \frac{\partial C}{\partial z} \qquad (2.4)$$

where J is the flux, $\mathcal{D}_{12}$, the diffusion coefficient and $\partial C/\partial z$ the concentration gradient.

The rate of change in concentrations in the top and bottom bulbs are given by:

$$\frac{dC_L}{dt} = -J(t)\frac{A}{V_L} \qquad (2.5a)$$

$$\frac{dC_0}{dt} = J(t)\frac{A}{V_0} \qquad (2.5b)$$

where J(t) is the diffusional flow as a function of time, A is the area of the bore in the connecting tube, V_L and V_0 are the volumes of the upper and lower bulbs respectively.

Combining eqns. (2.5a) and (2.5b):

$$\frac{d}{dt}(C_L - C_0) = -J(t)A\left(\frac{1}{V_L} + \frac{1}{V_0}\right) \tag{2.6}$$

Equation (2.4) is written as:

$$J(t) = \left(\frac{C_L - C_0}{L_{eff}}\right)\mathcal{D}_{12} \tag{2.7}$$

Substituting eqn. (2.7) into (2.6) gives:

$$\frac{-d\ell n(C_L - C_0)}{dt} = \frac{\mathcal{D}_{12}A}{L_{eff}}\left(\frac{1}{V_L} + \frac{1}{V_0}\right) \tag{2.8}$$

which becomes after integration:

$$C_L(t) - C_0(t) = \left(C_L^0 - C_0^0\right)\exp(-t/\tau) \tag{2.9a}$$

$$\tau = \left(\frac{\mathcal{D}_{12}A}{L_{eff}}\left(\frac{1}{V_L} + \frac{1}{V_0}\right)\right)^{-1} \tag{2.9b}$$

where C_L^0 and C_0^0 are the initial concentrations in the bulbs and τ is the so called "relaxation time".

Equation (2.9a) is that derived by Ney and Armistead.[11] The derivation involves the assumption of a quasi-stationary state, which implies a constant flux in the connecting tube and, therefore, a linear concentration gradient. (eqn. (2.7))
That is, for a given point in time:

$$J = -\mathcal{D}_{12}\frac{dC}{dz} = \text{constant} \tag{2.10}$$

A true quasi-stationary state actually exists only in the limit of a narrow connecting tube joining two infinitely large bulbs. In practice the concentra-

tion gradient does change along the connecting tube and it must be considered in the calculations.

Consider the flux at two positions, z and z + dz in the connecting tube:

$$J_z - J_{z+dz} = \mathcal{D}_{12}\left[\left(\frac{dc}{dz}\right)_z - \left(\frac{dc}{dz}\right)_{z+dz}\right] \qquad (2.11a)$$

whence

$$\frac{\partial C}{\partial t} = \mathcal{D}_{12}\frac{\partial^2 C}{\partial z^2} \qquad (2.11b)$$

Equation (2.11b) constitutes Fick's second law.

Colin Barnes[41] solved this flow equation, assuming the diffusion coefficient to be independent of concentration. His work was connected with mutual tracer diffusion in liquids using a diaphragm cell. The diaphragm is essentially many fine capillaries grouped together and results obtained are generally applicable to single capillary diffusion.

Further justification of this statement is given by Mason et al.[10]

In a publication by Mills and Woolf,[42] the results of the solution of Fick's second law for the diaphragm cell and for different initial conditions are summarized: Consider the following boundary conditions:

$$\frac{\partial C_L}{\partial t} = \frac{-\mathcal{D}_{12}A}{V_L}\left(\frac{\partial C_T}{\partial z}\right)_{z=L} \qquad (2.12a)$$

$$\frac{\partial C_0}{\partial t} = \frac{\mathcal{D}_{12}A}{V_0}\left(\frac{\partial C_T}{\partial z}\right)_{z=0} \qquad (2.12b)$$

where C_T is the concentration of gas in the connecting tube.

These two equations express the rate of change of

gas concentration in the bulbs.

Other boundary conditions are that

$$C_T(0,t) = C_0(t) \qquad (2.12c)$$

$$C_T(L,t) = C_L(t) \qquad (2.12d)$$

The solution was restricted to the conditions of equal bulb volumes and the ratio V_T/V_L (V_T being the volume of the connecting tube) made so small that second and third order terms in V_T/V_L were negligible.

Here reference is made to Ney and Armistead's[11] first assumption. Whereas the connecting tube volume was ignored in their derivation, Barnes[41] incorporated the volume in the term V_T/V_L. His solution takes the same form as eqn. (2.9a) with the relaxation time given by:

$$\tau = \left[\left(1 - \frac{V_T}{6V_L}\right)\frac{\mathcal{D}_{12}A}{L_{eff}}\left(\frac{1}{V_L} + \frac{1}{V_0}\right)\right]^{-1} \qquad (2.13)$$

Equation (2.13) differs from eqn. (2.9a) by the factor $(1 - V_T/6V_L)$, which is in fact a correction for the non-attainment of a quasi-stationary state.

Since the publication of Barnes[41] work, other workers have studied the problem of non-attainment of a quasi-stationary state without reference to his work.

Paul[43] gave a similar expression to eqn. (2.13) but obtained a factor of (1/4) instead of (1/6).

Annis et al.[44] treated the problem rigorously assuming that the mean flux in the connecting tube was proportional to the effective mean flux at the ends of the tube. An expression for the deviation from a quasi-

stationary state was developed and given by:

$$K = 1 + \frac{1}{3}\frac{V_T}{V_L}\left(\frac{1-\beta+\beta^2}{1+\beta}\right) \qquad (2.14)$$

$$\beta = V_L/V_0$$

In the special case of equal bulb volumes, this reduces to the same expression derived by Barnes:

$$K = 1 + \left(\frac{V_T}{6V_L}\right) \qquad (2.15)$$

$$\tau = \left(\frac{\mathcal{D}_{12}A}{KL_{eff}}\left(\frac{1}{V_L} + \frac{1}{V_0}\right)\right)^{-1} \qquad (2.16)$$

To correct for non equal bulb volumes in Barnes' solution of Fick's law, it has been shown that for small volume differences, (V_T/V_L) may be replaced by $(2\ V_T/(V_L+V_0))$.

For the cell considered in this work, the correction needed was small.

2.9 Relaxation Times

As mentioned previously, it was necessary to advance the connecting tube into the bulbs. This has the effect of reducing the bulb volumes. Each tube protruded 5.40 cm into each bulb. The diameter of the tube was 2.22 cm. Data from Tables (2.1) to (2.3) are summarized and the relaxation times calculated from eqn. (2.13) are given in the following table:

Table (2.5)

Relaxation Times for the Two Bulb Apparatus

	V_L (cm^3)	V_0 (cm^3)	r (cm)	L_{eff} (cm)	$1-\frac{AL_{eff}}{6V_L}$	$\tau \times 10^6$ (s)
1	5858.6	5803.4	0.2763	18.500	0.99987	4.4462
2	5858.6	5803.4	0.0535	69.032	0.99822	4.4651

2.10 *Errors*

Dimension measurements given in Tables (2.1) and (2.3) are the main sources of error in the relaxation time. A summary of these values is given below:

Table (2.6)

Errors in Dimension Measurements

	error length (%)	error radius (%)	error volume (%)	total error (%)
1	± 0.01	± 0.10	± 0.06	± 0.17
2	± 0.003	± 0.06	± 0.06	± 0.12

Errors arise from the correction factor for the non-attainment of a quasi-stationary state, but, as can be seen from Table (2.5), these are small. Some error is introduced by using the Wirz formula for the end correction. For the connecting tubes in this apparatus, the correction is close to that for the infinite flange, namely 0.82r and a maximum error of 0.05% would be introduced if this limiting value was used rather than the actual end correction.

Cathetometer readings of the meniscus of the silicone oil were reproducible to ± 0.002 cm, which would mean a maximum error in pressure measurements of 0.1%. Errors in density measurements were negligible. Each separate experiment was also subject to errors from the least square analysis and in general this did not exceed 0.1%.

Individual experiments would have a reproducibility of ±0.2%. The uncertainty of the diffusion coefficients is limited by the cell dimensions and in the correct choice of the end correction. If the correct end correction is used, data from different connecting tubes should overlap. Evidence of this will be given in Chapter IV.

From the data in Table (2.6), and the discussion that followed, the diffusion data should have an overall uncertainty of better than 0.2%.

2.11 Shearing Cell

The Shearing Cell is now discussed along similar lines. A diagram of this cell is given in fig. (2.2).

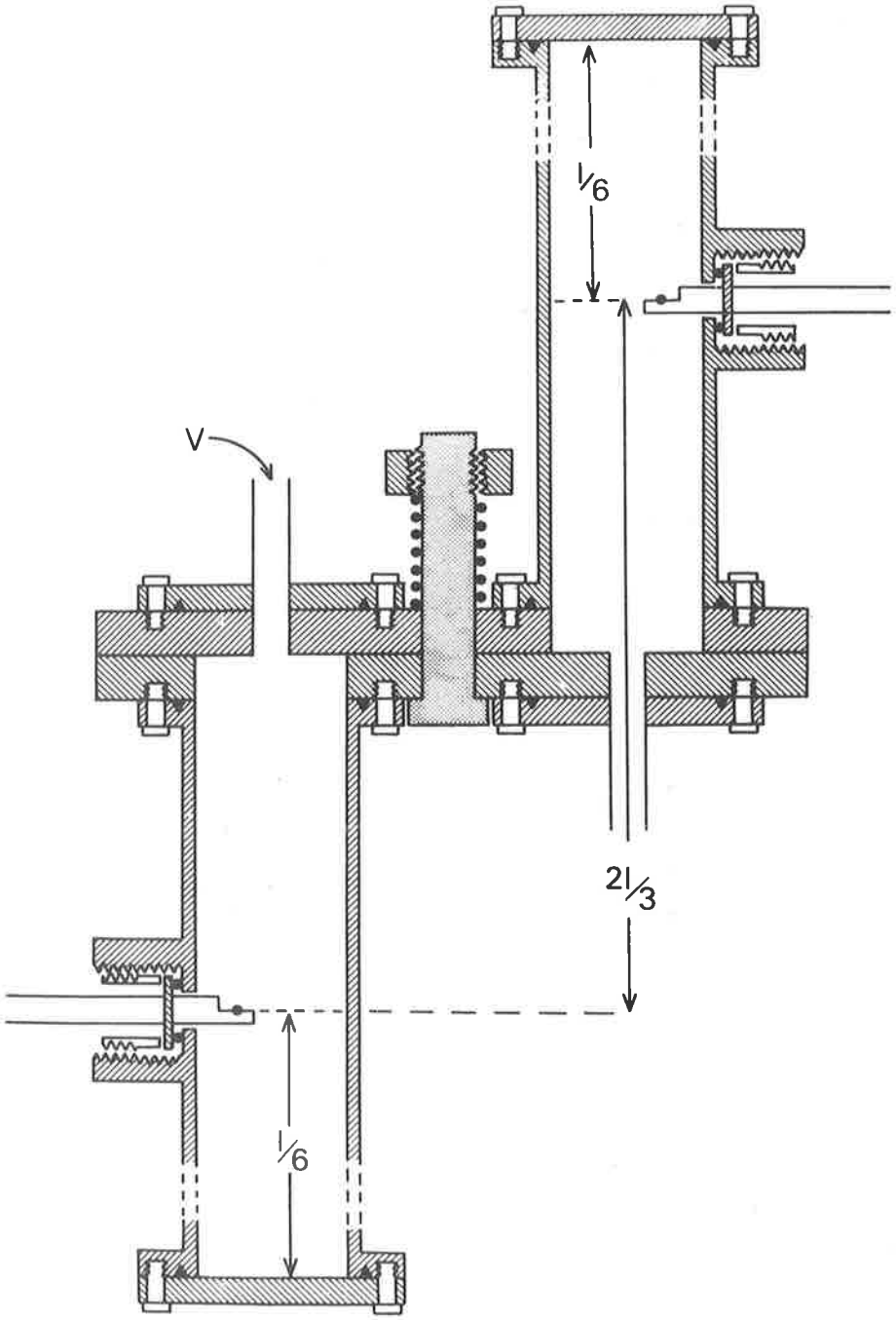

Fig. 2.2 The Shearing Cell.

It was constructed of two identical lengths of stainless steel tubing having internal diameters of 4.5 cm. These tubes were mounted on opposite sides of two stainless steel plates which rotate with respect to one another about a central pivot. Adjacent surfaces of the plates were lapped and Apiezon T-grease was used as a lubricant. These plates were compressed together by a spring which was tightened by a nut on the central pivot.

All seals were made with lead O-rings prepared in situ by moulding lead wire into V-shaped grooves. The design of these grooves was such that no dead space existed after compression. Matched thermistors were mounted at positions (L/6) from either end of the cell. As in the two bulb apparatus, the cell was suspended vertically in a water bath controlled to ± 0.001 K.

The top half of the cell was fixed and the bottom half was free to rotate through a restricted arc with a differential spur gear and pinion. The two halves of the cell could be rotated and brought into exact coincidence and also separated so that each half could be filled with a gas, or gas mixture, through ports, V.

Gas pressures were measured with a Bourdon Gauge (Texas Instrument, Houston) calibrated using a dead weight tester to an accuracy of 0.1%.

Both sides of the cell were filled to the same pressure so that no bulk flow of gas occurred when the two halves were brought into coincidence. Compositions were calculated using partial pressures. Experiments could be performed over the entire composition range using a successive dilution technique.

2.12 Theory

The flow equation for a shearing cell is Fick's second law, thus:

$$\frac{\partial C}{\partial t} = \mathscr{D}_{12}\frac{\partial^2 C}{\partial z^2} \qquad (2.17)$$

$$C = C(z,t)$$

with boundary conditions of no flow through the end plates.

$$\frac{\partial C(0,t)}{\partial z} = \frac{\partial C(L,t)}{\partial z} = 0 \qquad (2.18)$$

The solution[45] of eqn. (2.17) is:

$$C(z,t) = \sum_{n=0}^{\infty} B_n \cos\left(\frac{n\pi z}{L}\right)\exp(-n^2\pi^2\mathscr{D}_{12}t/L^2) \qquad (2.19)$$

The Fourier coefficients, B_n, are written in terms of half range cosine expansions:

$$B_0 = \frac{1}{L}\int_0^L F(z)dz \qquad (2.20a)$$

$$B_n = \frac{1}{L}\int_0^L F(z)\cos(n\pi z/L)dz \qquad (2.20b)$$

where F(z) are the initial conditions. In this type of cell they may be represented as:

$$\left.\begin{aligned} F(z) &= C_1^0 \\ F(z) &= C_2^0 \end{aligned}\right\} \quad \begin{aligned} &L/2<z<L \\ &0<z<L/2 \end{aligned}$$

where C_1^0 and C_2^0 are the initial concentrations in the top and bottom compartments respectively.

Evaluating eqns. (2.20) gives:

$$B_0 = C(\infty) \tag{2.21a}$$

$$B_n = \frac{2(C_1^0 - C_2^0)}{n\pi} \sin(n\pi/2) \tag{2.21b}$$

Substituting into eqn. (2.19):

$$C(z,t) = C(\infty) + \frac{2(C_1^0 - C_2^0)}{\pi} \sum_{n=1}^{\infty} \frac{1}{n} \sin(n\pi/2)$$

$$\times \cos\left(\frac{n\pi z}{L}\right) \exp(-n^2\pi^2 \mathcal{D}_{12} t/L^2) \tag{2.22}$$

Positioning the thermistors at positions (L/6) and (5L/6) along the cell and taking differences in concentration gives:

$$\Delta C = \frac{2\sqrt{3}}{\pi} (C_1^0 - C_2^0) \exp(-t/\tau) \tag{2.23a}$$

$$\tau = \frac{L^2}{\pi^2 \mathcal{D}_{12}} \tag{2.23b}$$

Higher terms that should appear in eqn. (2.23a) become negligible after an initial period of time.

2.13 Concentration dependence of the Diffusion Coefficient

In the solution of Fick's second law for both the two bulb apparatus and the shearing cell, the diffusion coefficient was assumed independent of concentration. In fact diffusion coefficients of gases may vary as much as 5% over the entire concentration range, but over the range of measurement, this variation is approximately

linear. Therefore Fick's second law should be written as:

$$\frac{\partial C}{\partial t} = \frac{\partial}{\partial z}\left(\mathcal{D}_{12}\frac{\partial C}{\partial z}\right) \qquad (2.24)$$

and the diffusion coefficient given by:

$$\mathcal{D}_{12} = D_0 + CD_1 \qquad (2.25)$$

Ljunggren[45] has solved eqn. (2.24) assuming a linear change in diffusion coefficient and arrived at the result:

$$\tau = L^2/\pi^2(D_0+C(\infty)D_1) \qquad (2.26)$$

$$= L^2/\pi^2\mathcal{D}_{12}^m$$

Equation (2.26) implies that the measured diffusion coefficient is simply the one at the final concentration $C(\infty)$.

2.14 Comparison between the two Cells

The shearing cell has the advantage of having one dependent dimension, the length of the cell, which may be measured very accurately. In the two bulb apparatus, uncertainties, which have been summarized in section (2.10), are introduced. Assumptions made in the solution of Fick's second law for the shearing cell are:

(i) Uniform cross sectional area.

(ii) Symmetry about the central plates.

(iii) The diffusion coefficient is concentration independent.

Errors from (i) and (ii) are minimized by careful

design and construction and (iii) has been discussed in section (2.13).

The main disadvantages of the shearing cell are effects that occur because the gases are not ideal:

(i) Dufour effect.

(ii) Heat of mixing.

The Dufour effect is a small temperature transient that occurs when two gases interdiffuse. Ljunggren[45] has developed an expression for these two effects by solving a differential equation derived by Waldmann.[46-48]

The solution given by Ljunggren can be approximated to:

$$\nu_1 = \frac{8}{\pi}\theta_\alpha\phi(y)(-0.866\ \exp(-t/\tau)) + \frac{32}{\pi^3}\theta_B\phi(y)(\tfrac{1}{4}\exp(-2t/\tau)-\tfrac{1}{2}\exp(-10t/\tau)) \quad (2.27a)$$

$$\nu_2 = \frac{8}{\pi}\theta_\alpha\phi(y)(+0.866\ \exp(-t/\tau)) + \frac{32}{\pi^3}\theta_B\phi(y)(\tfrac{1}{4}\exp(-2t/\tau)-\tfrac{1}{2}\exp(-10t/\tau)) \quad (2.27b)$$

where ν_1 and ν_2 are the temperature transients at the top and bottom thermistors respectively, and

$$\theta_\alpha = (\frac{2r}{L})^2 \frac{\mathcal{D}_{12}}{\lambda} (C_1^0 - C_2^0)\ \delta T_\alpha \quad (2.28a)$$

$$\theta_B = (\frac{2r}{L})^2 \frac{\mathcal{D}_{12}}{\lambda} (C_1^0 - C_2^0)^2\ \delta T_B \quad (2.28b)$$

$$\phi(y) = \sum_{m=0}^{\infty} \frac{(-1)^m}{(2m+1)^3} \cos(\frac{(2m+1)\pi y}{2r}) \quad (2.28c)$$

$$\delta T_\alpha = \alpha'(R/C_p)T \quad (2.28d)$$

$$\delta T_B = b^* (R/C_p) T/\tilde{V} \qquad (2.28e)$$

α' is the thermal diffusion factor, λ the thermal conductivity of the gas mixture, C_p the heat capacity, $\tilde{V}$ the molar volume of the gas, b^* a function of the virial coefficients and $\phi(y)$ is a function dependent upon the position along the diameter of the cell. The value of this factor is a maximum along the central axis of the cell ($y = 0$) and is of the order of one.

The first term in eqns. (2.27) gives rise to the Dufour effect and the second term to the "heat of mixing". Considering only the "heat of mixing" term:

$$\begin{aligned} \Delta\nu &= (\nu_1 - \nu_2) \\ &= \frac{8}{\pi^3} (c_1^0 - c_2^0)^2 \phi(y) \left(\frac{2r}{L}\right)^2 \mathcal{D}_{12} \delta T_B \\ &\quad \times \left(\frac{1}{\lambda_1} - \frac{1}{\lambda_2}\right) \exp(-2t/\tau) \end{aligned} \qquad (2.29)$$

where subscripts 1 and 2 refer to the top and bottom halves of the cell respectively.

It will be shown in Chapter III that $\left(\frac{1}{\lambda_1} - \frac{1}{\lambda_2}\right)$ decays as $\exp(-t/\tau)$ and, therefore, the contribution from the heat of mixing should decay as $\exp(-3t/\tau)$ and, therefore becomes negligible after a period of time.

Now consider the contribution due to the Dufour effect:

$$\begin{aligned} \Delta\nu &= (\nu_1 - \nu_2) \\ &= -\frac{6.93}{\pi} (c_1^0 - c_2^0) \phi(y) \left(\frac{2r}{L}\right)^2 \mathcal{D}_{12} \\ &\quad \times \delta T_\alpha \left(\frac{1}{\lambda_1} + \frac{1}{\lambda_2}\right) \exp(-t/\tau) \end{aligned} \qquad (2.30)$$

It is interesting to note that the Dufour effect is negative at the top thermistor and positive at the bottom thermistor, whereas the heat of mixing is positive at both positions.

In eqn. (2.30) the term $\left(\frac{1}{\lambda_1} + \frac{1}{\lambda_2}\right)$ is essentially constant during an experiment (Chapter III) and, therefore, Dufour contributions decay at the same rate as diffusion. Diffusion data,[49] using diffusion cells of different lengths and cross-sectional areas, show no detectable difference in the measured diffusion coefficient.

Both of these effects exist in the two bulb apparatus but should not interfere with the diffusion measurements. Diffusion is restricted to the connecting tube and, therefore, any transient heat generated will be dissipated before reaching the thermistors.

From a first glance it would appear that the shearing cell results would be the more accurate because the relaxation time depends upon the single length measurement. Upon closer examination, the shearing cell reveals problems that may be difficult to determine and to correct. It is important then to analyse each experiment critically and try to determine which, if any, of these effects are causing problems. The discussion will be resumed in Chapter IV.

CHAPTER III

DIFFUSION BRIDGE ANALYSIS

3.1 Introduction

Determination of diffusion coefficients, using the type of cells considered in Chapter II, depends upon being able to accurately measure changes in gas concentrations as a function of time. Analysis of such data reduces to a determination of the relaxation time defined in the previous chapter.

Two electrical circuits, incorporating the two thermistors, will be discussed and it will be shown how the difference in resistance, ΔR, measured as a function of time for one of these circuits, conveniently gives access to the diffusion coefficient. The reason for this is, as will be shown, a fairly exact proportionality between ΔR and the difference in concentration ΔC.

The thermistors used were Fenwal G112P (Fenwal Electronics, Framingham, Massachusetts) being metallic oxide beads encased in a glass envelope. These particular thermistors are sold in pairs by the manufacturer and matched to within certain standards. At 25°C the thermistors should be 8000Ω and matched to within 0.7% of each other when in an environment of helium. The mismatching gives rise to the residual $\Delta R(\infty)$ term in the expression for ΔR as a function of time. (See eqn. (3.5))

The temperature dependence of a thermistor[50] may be given by:

$$R_T = R_{T_w} \exp\left[B\left(\frac{1}{T} - \frac{1}{T_w}\right)\right] \qquad (3.1)$$

T being the thermistor temperature, T_w the temperature of the water bath, R_w the thermistor resistance at the temperature, T_w, and B a characteristic constant, the magnitude depending upon the particular thermistor material. For Fenwal G112P thermistors the value is approximately 4000K.

For small temperature changes, eqn. (3.1) simplifies to:

$$R_T = R_w - \frac{BR_w}{T_w^2}(T - T_w) \qquad (3.2)$$

implying a linear dependence upon the temperature gradient between the thermistor and surrounding gas.

3.2 Circuit Analysis

Circuit A

In this circuit (illustrated fig. (3.1)) R_1 and R_2 are the two thermistors, R_3 and R_4 are matched 5000Ω micacard resistors, R_5 is a precision variable resistance box (Dekabox DB62, Electro Scientific Industries, Portland, Oregon) and V is a constant potential difference applicable at all times across the circuit.

During the course of the experiment, R_5 is continually adjusted so that V_{24} is nulled, implying that:

$$\Delta R(t) = R_5 = (R_1 - R_2) \qquad (3.3)$$

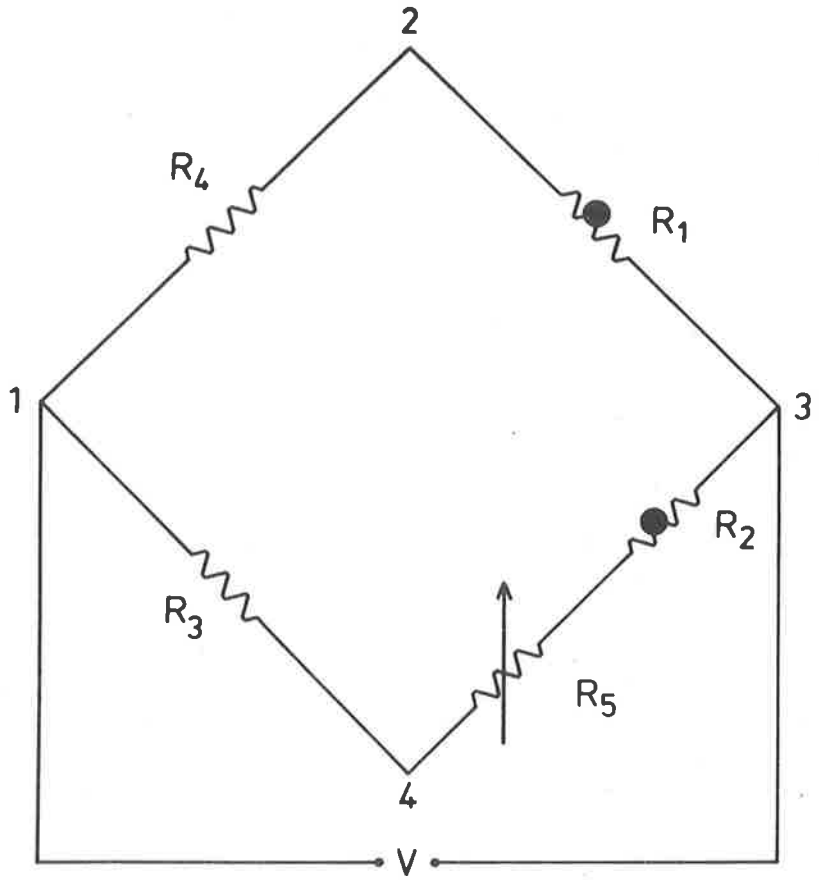

Fig. 3.1 The Wheatstone Bridge Circuit.

R_5 is then a convenient measure of ΔR at any time during the experiment.

Circuit B

This circuit is as above except for the omission of R_5. In this case the difference in resistance ΔR produces a measurable voltage V_{24} between the two arms of the bridge.

Circuit analysis (Appendix II) shows that:

$$\Delta R(t) = \frac{R_3 \, V \, V_{24}}{V_{14}(V_{14}-V_{24})} \qquad (3.4)$$

This result is subject to the conditions of matched resistors R_3 and R_4 and a constant controlled voltage, V.

At regular time intervals accurate determination of voltages V_{24} and V_{14} are required. During an experiment both output voltages are connected to separate channels of an analogue scanner, which in turn is interfaced to a digital voltmeter. (Solartron, Schlumberger) A crystal timer, designed to produce a pulse at preset time intervals, initiates a scan and the output voltages are simultaneously recorded on either paper tape (Facit) or a mechanical printer (Hewlett-Packard).

In practice the voltage V_{14} changes slowly with time and, therefore, negligible error is incurred by recording its measurement immediately after voltage V_{24}. A direct proportionality is assumed between the difference in resistance and the difference in concentration at the two thermistor positions, so results for both circuits are

fitted, by the method of least-squares,[38] to the function:

$$\Delta R(t) = \Delta R(\infty) + A\exp(-t/\tau) \qquad (3.5)$$

where $\Delta R(\infty)$ is the residual resistance due to mixmatching of the thermistors, A is a constant and τ is the same relaxation time found in eqns. (2.9a) and (2.23a).

3.3 Power Considerations

At any time during a diffusion experiment the temperature of each thermistor is a function of the heat energy contained therein. Energy is supplied by the passage of electric current and dissipated by the surrounding gas and secondary losses, such as conduction along the thermistor supports.

The rate of heat energy transfer depends upon the thermal conductivity of the surrounding gas and the temperature gradient operating about the thermistor. Convective effects are assumed to be negligible. Ambient temperature is held constant (to within ± 0.001K) by the surrounding water bath.

Thus the power dissipated may be expressed as:

$$P_i = a_1\lambda_i(T_i-T_w) + a_2(T_i-T_w) \qquad (3.6)$$

$$i = 1,2$$

λ_i being the thermal conductivity of the gas about the i^{th} thermistor and a_1 and a_2 are constants.

The first term represents energy losses to the gas mixture, while the second term accounts for losses such as conduction along the wire supports.

Combining eqn. (3.2) with eqns. (3.6) yields an

expression for the thermistor in terms of the thermal conductivity of the gas and the power input.

$$R_i = R_w + \frac{\xi P_i}{(\lambda_i+\delta)} \qquad i = 1,2 \qquad (3.7)$$

where $\xi = (-BR_w/a_1T_w^2)$

$$\delta = (a_2/a_1)$$

In principle the constant, ξ, could be calculated, but because of the uncertainty in estimating a_1,[51] it is used as a scaling factor to correlate experimental and calculated $\Delta R(t)$ values.

A theoretical expression for $\Delta R(t)$ may be derived from eqns. (3.7):

$$\Delta R(t) = (R_1-R_2) = \xi\left(\frac{P_1}{\kappa_1} - \frac{P_2}{\kappa_2}\right) \qquad (3.8)$$

where $\kappa_i = (\lambda_i+\delta)$ could be termed an *effective thermal conductivity*.

3.4 Analysis

This analysis will show that for Circuit B at all times during the course of the diffusion experiment ΔR is approximately proportional to the concentration difference, ΔC.

Both the power input and thermal conductivity of the gas mixture depend upon the concentration and, therefore they may be written in the form:

$$\kappa = f_\kappa(C)$$

$$P = f_P(C)$$

Expanding these quantities as a Taylor series yields:

$$\kappa_i = f_\kappa(\bar{C}) + f'_\kappa(C_i-\bar{C}) + \frac{f''_\kappa}{2!}(C_i-\bar{C})^2 + \ldots.$$

$$P_i = f_P(\bar{C}) + f_P(C_i-\bar{C}) + \frac{f''_P}{2!}(C_i-\bar{C})^2 + \ldots.$$

$$\bar{C} = (C_1+C_2)/2 \qquad (3.9)$$

$f_\kappa(\bar{C})$ and $f_P(\bar{C})$ are the thermal conductivity and power, respectively corresponding to the mean concentration, $\bar{C}$, and f'_κ, f''_κ, f'_P and f''_P are the derivatives with respect to concentration.

Substituting into eqn. (3.8) gives, after several manipulations:

$$\Delta R(t) = H(C_1-C_2)(1-M(C_1-C_2)^2) \qquad (3.10)$$

$$+ \text{(higher order terms)}$$

$$H = \left(\xi/f_\kappa^2(\bar{C})\right)(f'_P(\bar{C})f_\kappa(\bar{C})-f_P(\bar{C})f'_\kappa(\bar{C}))$$

$$M = \left(f_\kappa(\bar{C})f''_\kappa(\bar{C})-(f'_\kappa(\bar{C}))^2\right)/4f_\kappa^2(\bar{C})$$

In other words, the difference in resistance is approximately proportional to the concentration difference, since the next highest term depends upon $(\Delta C)^3$ which is negligible for experiments in this work.

It is important to note that eqns. (3.9) are only applicable to Circuit B. The presence of R_5 in Circuit A introduces an assymetry into $f_P(C)$ and the simplification of eqn. (3.10) does not apply. This results in a non-proportionality of ΔR and ΔC, thus

invalidating the use of this circuit in the determination of diffusion coefficients.

In the following section another analysis method is considered. Diffusion experiment will be simulated using eqn. (3.8) for both circuits. It will be shown that results are in agreement with the analysis of this section.

3.5 Further Method of Analysis

Using eqn. (3.8) it is possible to obtain ΔR as a function of time by mathematical calculation, knowing how the gases should behave ideally. Apart from the constant, ξ, the only unknown in this equation is δ, which may be determined in the following manner:

Corresponding values of R_i and P_i for a *single* thermistor in different concentrations of surrounding gas are obtained. R_i was obtained with a resistance box in the opposite arm of the bridge (fig. 3.1) and the power by knowing the voltage applied across the circuit.

From eqn. (3.7) a plot of R_i versus P_i gives a linear relationship, the slope of which is the quantity $(\xi/(\lambda_i+\delta))$. The slope of such a plot changes with concentration as λ_i varies.

Literature values for the concentration dependence of the thermal conductivity are necessary and from this data, choosing a particular concentration as a reference, the ratios $(\lambda_i/\lambda_{ref})$ may be formed.

A value of δ can be found such that $(\lambda_i+\delta)/(\lambda_{ref}+\delta)$ equals the ratio of slopes formed from the above experiments, this time using the slope at the concentration

chosen above as reference.

A typical plot for the system He/Ar, using the data of Van Dael of Cauwenbergh,[52] is presented in fig. (3.2). Calculations indicate that the choice of δ is not critical.

For given initial conditions and an experimental relaxation time, the concentration at each thermistor position may be calculated from eqn. (2.22), at any time, t.

At a particular time, the thermal conductivity is derived from the reference data relating λ_i to concentration. Since the constants ξ and δ are known, only the power through the thermistor needs to be calculated in order to obtain the thermistor resistances at any time during the experiment. However, the power depends upon the thermistor resistance and, therefore, an iterative procedure is employed.

For a given bridge voltage and an estimated value of the thermistor resistances at the end of the experiment, (assumed perfectly matched) the power through each thermistor may be calculated. In turn this may be substituted into eqn. (3.7) to obtain a second approximation to the resistance which is used to re-evaluate the power. This procedure is repeated until convergence.

Thus at any time, t, values of R_i may be found. The difference ΔR may be found by subtraction and tabulated as a function of time.

Fitting this data to the eqn. (3.5) by the method of least squares, should result in a relaxation time, τ, indistinguishable from the experimental value.

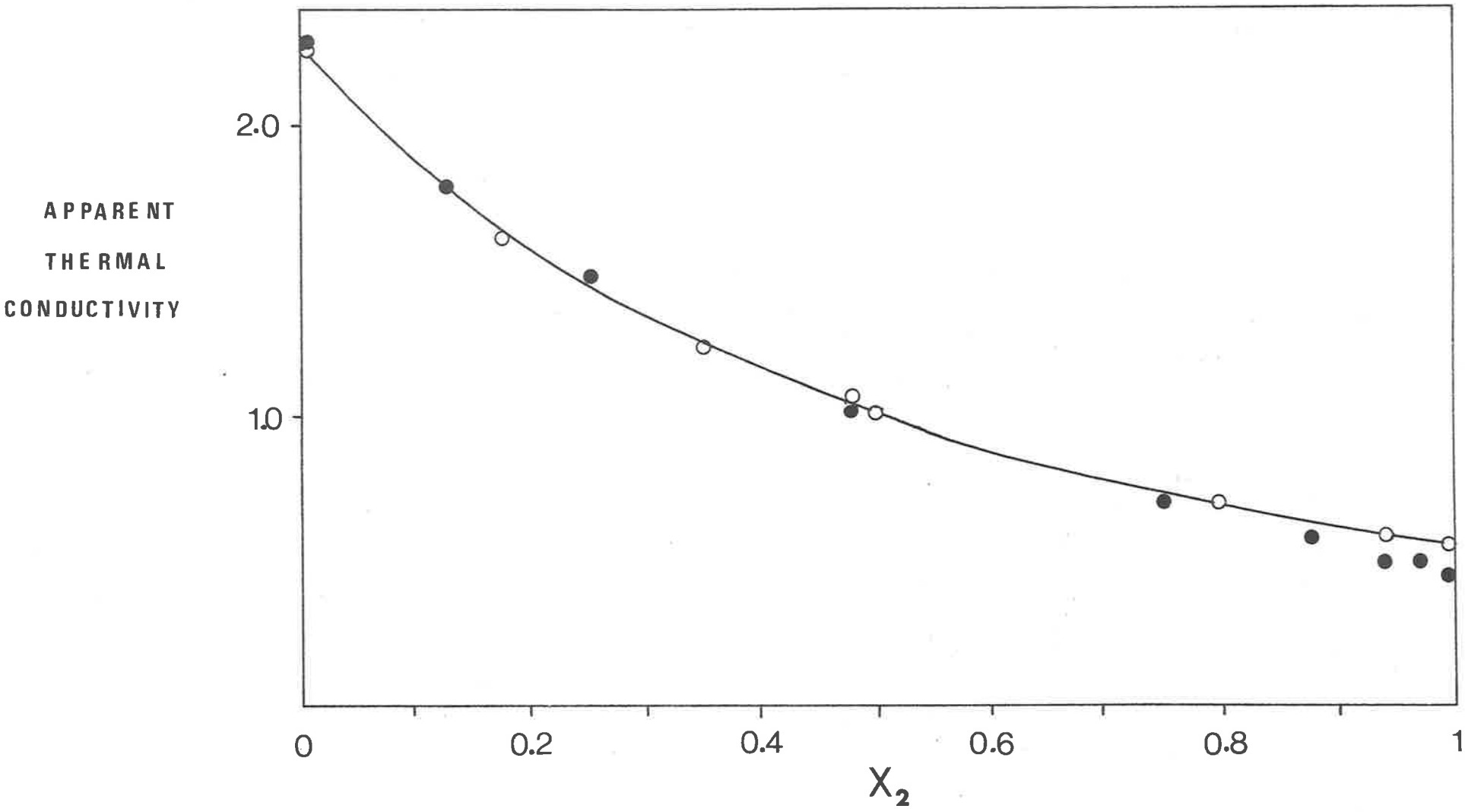

Fig. 3.2 Plot of Apparent Thermal Conductivity as a Function of Concentration for the system He/Ar.

● - $(\lambda_i/\lambda_{ref})$ - Experimental Values. ○ - $(\lambda_i+\delta)/(\lambda_{ref}+\delta)$ - Literature Values.

In the case of Circuit B, this is the situation, but in Circuit A the presence of the resistance box, R_5, changes the power input in the lower thermistor and this reflects in a spurious value for the relaxation time.

Results for both circuits will be discussed in Chapter IV.

CHAPTER IV

RESULTS AND DISCUSSION

4.1 Diffusion Circuit Analysis

The analysis methods employed in Chapter III indicated that Circuit B should be used when measuring binary diffusion coefficients. In the following discussion, the concentration dependence of the He/Ar system, measured with the shearing cell, at one atmosphere pressure and 300K will be considered.

The results[8] for Circuit A are presented in Table (4.1) and those of Circuit B in Table (4.7). A difference in the diffusion coefficient between the two methods of measurement is indicated. To theoretically predict such a difference, the analysis method given in section (3.5) is employed.

Results for Circuit A:

A diffusion experiment was simulated according to the method described in section (3.5). This data was then fitted to eqn. (3.5) by the method of least-squares.[38]

Calculated least-square parameters were found to disagree with the experimental quantities which were defined when the simulated experiment was created. In the case of the relaxation time, deviations of up to 0.7% were observed.

Table (4.1)

Results for the system He/Ar at 300K using Circuit A

Corrections for power effects

x_2	$(P\mathcal{D}_{12})$ $(atm.cm^2.S^{-1})$	$(P\mathcal{D}_{12})_{corr}$ $(atm.cm^2.S^{-1})$
0.075	0.7373	0.7400
0.083	0.7373	0.7402
0.130	0.7379	0.7413
0.143	0.7408	0.7428
0.255	0.7419	0.7459
0.500	0.7505	0.7528
0.500	0.7498	0.7524
0.750	0.7558	0.7576
0.746	0.7545	0.7576
0.871	0.7556	0.7595
0.934	0.7564	0.7607

By progressively omitting the initial data points from the simulated experiment, each occasion fitting to eqn. (3.5), an increase in the relaxation time was observed. A plot of the calculated relaxation time versus the number of ohms out of balance was found to be linear, the intercept being the experimental quantity.

The parameter, $\Delta R(\infty)$, showed the same linear dependence upon the number of ohms out of balance.

Trends predicted in this model are observed in actual experiments. In the case of the parameter, $\Delta R(\infty)$, predicted deviations were of the order of 0.02Ω, which was considered the experimental uncertainty in this quantity.

A method of correcting the experimental results obtained from this circuit is as follows: For each experiment the maximum number of ohms out of balance is determined. Deviations from the true relaxation time may be found from a plot of the predicted relaxation time as a function of the out of balance.

In this manner corrections to the data have been made and the results are given in Table (4.1).

Results for Circuit B

Employing the same analysis procedure as for Circuit A reveals no significant deviations between the experimental and calculated least-square parameters of eqn. (3.5).

Actual experiments, obtained using this circuit, show none of the variations observed in Circuit A results.

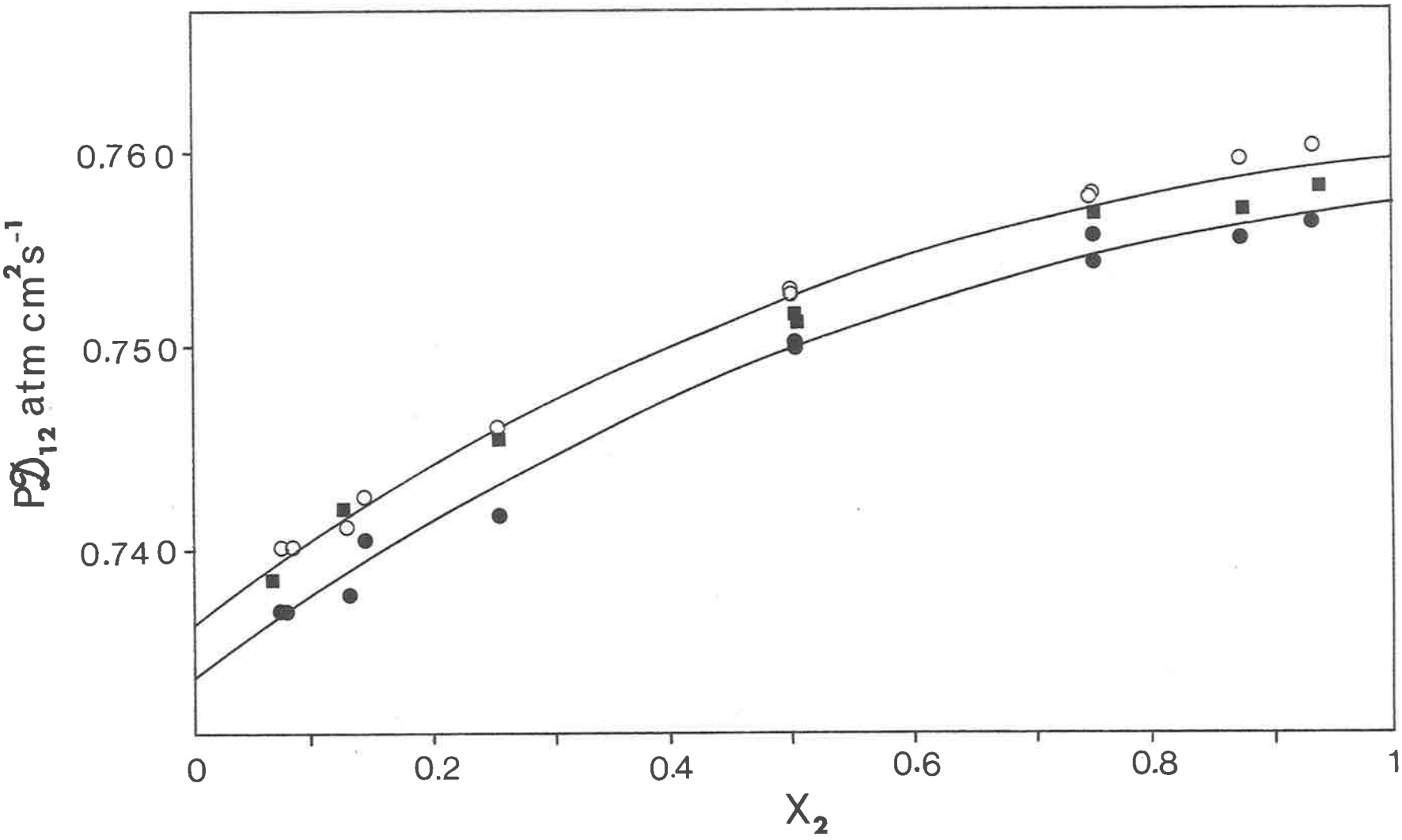

Fig. 4.1 Comparison between Diffusion Coefficient Results obtained using Circuit A and Circuit B.

■ - Circuit B ● - Circuit A ○ - Corrected Results for Circuit A

Summary

The findings of this analysis are summarized in fig. (4.1). Given are the two experimental data sets and the corrected results for Circuit A. There is excellent agreement between the Circuit B data and the results of Circuit A after appropriate corrections have been made.

This comparison between experimental results and predictions based upon the analysis of section (3.5) vindicates the conclusions of Chapter III, namely the direct proportionality between the difference in resistance between the two thermistors and the concentration difference at the thermistor positions for Circuit B and also the disturbing effect the resistance box has upon the system in Circuit A.

4.2 Two Bulb Apparatus Results

In Tables (4.2) and (4.3) diffusion coefficients for the systems He/Ar and He/O_2 at 300K and as a function of $(Pr)^{-1}$ are presented. Results for each system are given at three different mole fractions. Small corrections to the data (less than 0.1%) were sometimes necessary to adjust the result to the chosen mole fraction.

Graphical representation of the results is given in figs. (4.2) and (4.3).

Equation (1.18) describes the behaviour of a diffusing gas mixture at a pressure, P, and in a capillary of radius, r. However, for the two bulb apparatus considered here, eqn. (1.19) is sufficient to describe the results.

Table (4.2)

Diffusion Coefficients for the system He/Ar at 300K as a function of $(Pr)^{-1}$

P($x10^3$) (atm)	$(Pr)^{-1}$ $(atm.cm)^{-1}$	(PD_{12}) $(atm.cm^2.s^{-1})$
	$x_2 = 0.1$	
8.071*	231	0.7365
6.557*	285	0.7361
6.335*	295	0.7352
5.906*	316	0.7353
10.444	347	0.7350
7.810	463	0.7334
7.039	514	0.7323
6.485	558	0.7309
3.172*	589	0.7310
5.605	646	0.7302
5.048	717	0.7282
3.861	937	0.7256
3.780	957	0.7248
	$x_2 = 0.58$	
9.591	377	0.7517
8.230	440	0.7510
6.666	543	0.7498
5.111	708	0.7489
4.018	901	0.7463

Table (4.2) (Continued)

$P(\times 10^3)$ (atm)	$(Pr)^{-1}$ $(atm.cm)^{-1}$	(PD_{12}) $(atm.cm^2.s^{-1})$
	$x_2 = 0.9$	
7.089*	264	0.7594
6.184*	302	0.7593
10.390	348	0.7589
4.903*	381	0.7595
4.384*	426	0.7591
7.711	469	0.7583
6.034	600	0.7568
5.875	616	0.7578
4.351	832	0.7576
4.329	836	0.7565
3.781	957	0.7547
3.683	983	0.7558

*The experiments were performed with the connecting tube with r = 0.5353 cm.

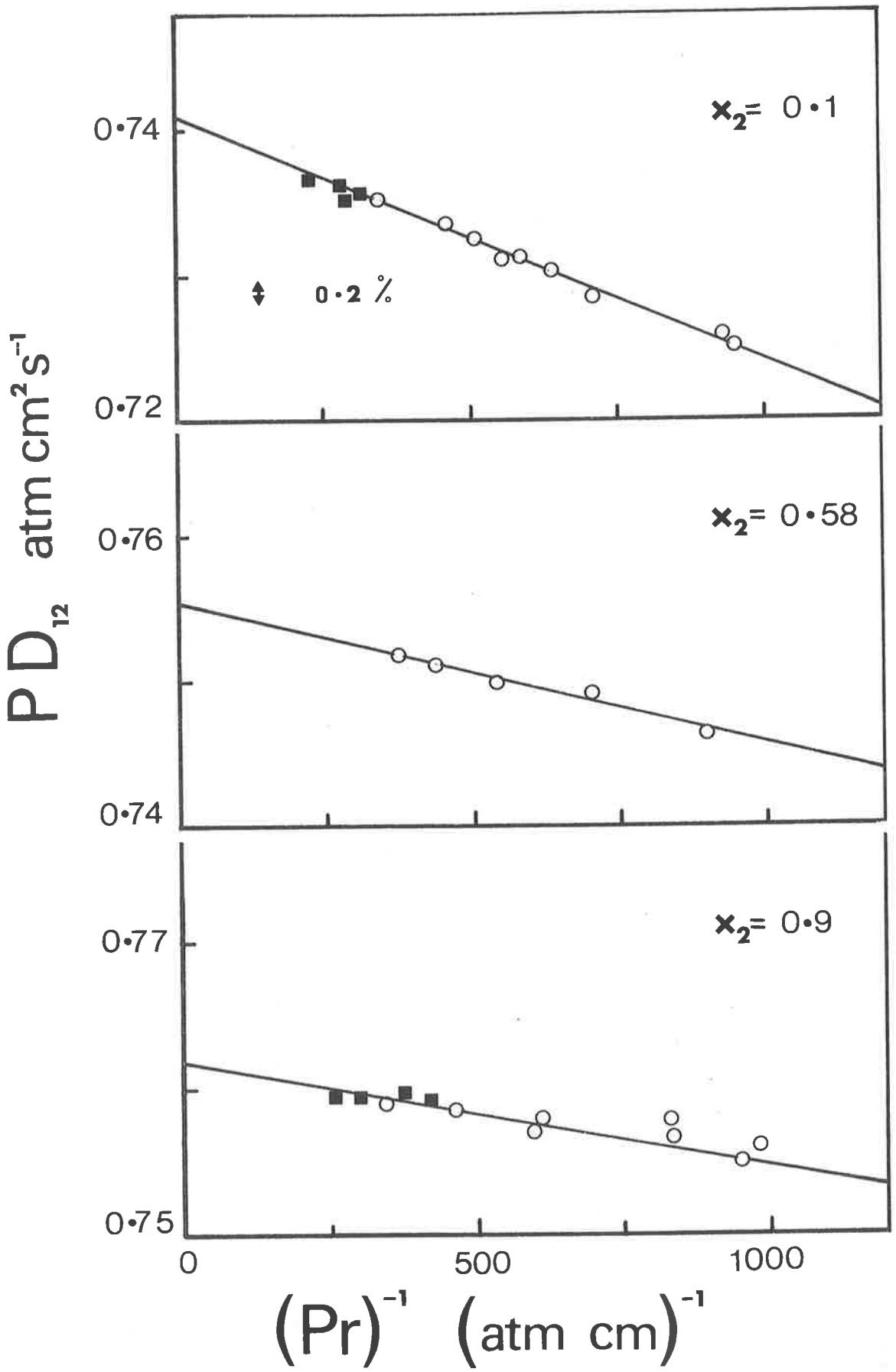

Fig. 4.2 (PD_{12}) as a function of $(Pr)^{-1}$ for the system He/Ar at 300K.

■ - r = 0.5353 cm. ○ - r = 0.2763 cm.

Table (4.3)

Diffusion Coefficients for the system He/O_2 at 300K as a function of $(Pr)^{-1}$

P(x10^3) (atm)	$(Pr)^{-1}$ $(atm.cm)^{-1}$	(PD_{12}) $(atm.cm^2.s^{-1})$
	x_2 = 0.1	
7.146*	261	0.7493
5.918*	316	0.7476
5.810*	322	0.7486
10.280	352	0.7484
4.916*	380	0.7469
4.867*	385	0.7475
7.706	470	0.7457
7.604	476	0.7451
5.814	623	0.7434
2.972*	629	0.7435
2.973*	629	0.7443
4.507	802	0.7426
4.485	807	0.7409
4.132	876	0.7409
3.607	1003	0.7404
3.361	1077	0.7391
	x_2 = 0.25	
7.696*	243	0.7544
6.563*	285	0.7546
5.664*	330	0.7542
5.657*	330	0.7544

Table (4.3) (Continued)

$P(x10^3)$ (atm)	$(Pr)^{-1}$ $(atm.cm)^{-1}$	(PD_{12}) $(atm.cm^2.s^{-1})$
	$x_2 = 0.25$	
4.954*	377	0.7530
9.271	390	0.7527
4.477*	418	0.7534
7.099	510	0.7513
6.969	519	0.7510
5.496	659	0.7491
5.280	685	0.7505
5.029	720	0.7486
4.466	810	0.7490
4.050	894	0.7465
	$x_2 = 0.9$	
7.113*	263	0.7671
5.906*	316	0.7671
5.829*	321	0.7662
10.350	350	0.7666
4.438*	421	0.7663
5.921	611	0.7649
4.956	730	0.7638
3.730	970	0.7617
3.374	1073	0.7614

*The experiments were performed with the connecting tube with r = 0.5353 cm.

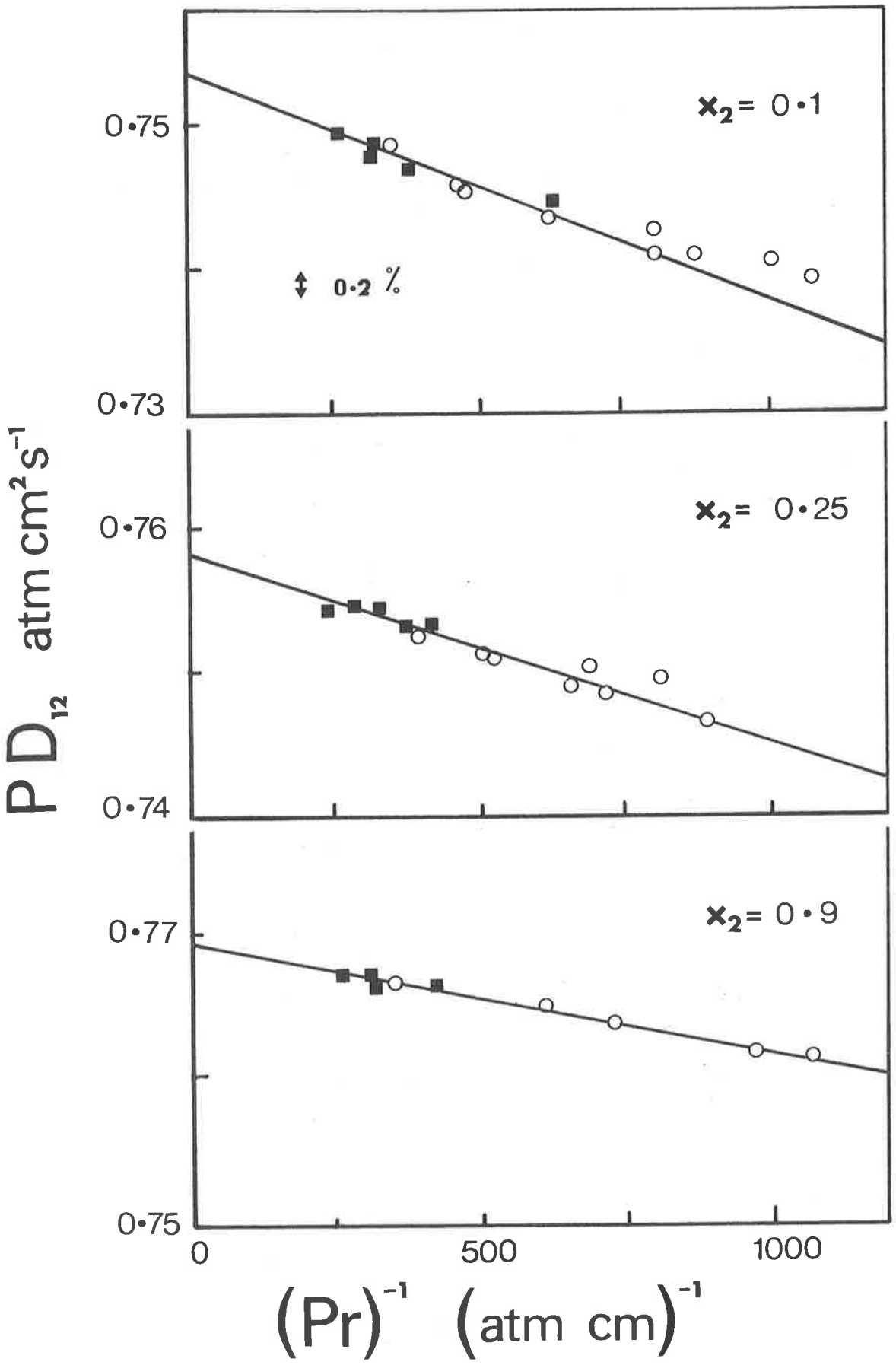

Fig. 4.3 (PD_{12}) as a function of $(Pr)^{-1}$ for the system He/O_2 at 300 K.

■ - r = 0.5353 cm. ○ - r = 0.2763 cm.

Using ($P\mathcal{D}_{12}$) as the only variable, the lines shown in figs. (4.2) and (4.3) are obtained by minimization of the residuals between experimental and predicted results. Optimum values of the intercept and the limiting slope $-B(P\mathcal{D}_{12})$ are given in Table (4.4) below:

Table 4.4

Comparison of Parameters obtained from eqn. (1.19) and those of a Least-Squares Analysis of the data

	Eqn. (1.19)		Least-square Parameters Eqn. (1.11)	
x_2	$(P\mathcal{D}_{12})$	$(-BP\mathcal{D}_{12})\times10^5$	$(P\mathcal{D}_{12})$	$(-C_2P\mathcal{D}_{12})\times10^5$
		He/Ar		
0.1	0.7407	1.698	0.7404±0.0006	1.617±0.096
0.58	0.7552	0.952	0.7554±0.0016	0.984±0.255
0.9	0.7620	0.723	0.7611±0.0010	0.559±0.163
		He/O_2		
0.1	0.7535	1.616	0.7518±0.0009	1.222±0.146
0.25	0.7583	1.329	0.7578±0.0010	1.215±0.182
0.9	0.7693	0.753	0.7691±0.0005	0.731±0.087

Also presented in Table (4.4) are the parameters obtained from fitting the data in Tables (4.2) and (4.3) to eqn. (1.11) by the method of least-squares.[38] Errors quoted are the 95% confidence limits.

In all cases, excepting He/O_2 at $x_2 = 0.1$, the intercept values agree, within the experimental error. If the data points at $(Pr)^{-1}$ equal to 1003 and 1077 $(atm.cm.)^{-1}$ are omitted from the analysis of this set of results, the two intercept values are in agreement.

Writing eqn. (1.19) in the form of eqn. (1.20) gives access to the extrapolated diffusion coefficients at any mole fraction.

Data for the two systems as a function of mole fraction are presented in Tables (4.5) and (4.6). The values of $(Pr)^{-1}$ are given and the results have been extrapolated to yield the intercept $(P\mathcal{D}_{12})$.

Results for the experiments performed with the two connecting tubes, characterised in Chapter II, show excellent agreement. This is well illustrated by the overlap of the respective data. (refer figs. (4.2) and (4.3))

In the case of the concentration dependence, the results obtained from the two connecting tubes are indistinguishable. (figs. (4.4) and (4.5))

These indicate that the correct end correction to the connecting tube has been assigned and also the corrections made for the non-attainment of a quasi-stationary state appear to be of the right order of magnitude.

Equation (1.19), derived from the results of the dusty gas model, describes the behaviour of a diffusing gas in a capillary at low values of $(Pr)^{-1}$ extremely well. The composition and pressure dependence of the diffusion coefficient are predicted to within the uncertainty of

Table (4.5)

Two Bulb Apparatus Results for the Concentration Dependence of the Diffusion Coefficient for the system He/Ar at 300K

x_2	P (atm)	$(Pr)^{-1}$ $(atm.cm)^{-1}$	(PD_{12}) $(atm.cm^2.s^{-1})$	$(P\mathcal{D}_{12})$ $(atm.cm^2.s^{-1})$
0.071	5.436	666	0.7262	0.7380
0.075	4.087	886	0.7244	0.7401
0.125*	4.046	462	0.7346	0.7421
0.215	4.366	829	0.7337	0.7455
0.218*	4.526	413	0.7409	0.7468
0.288*	4.973	376	0.7420	0.7469
0.355*	5.490	340	0.7456	0.7497
0.423*	6.131	305	0.7482	0.7516
0.593	5.721	633	0.7501	0.7561
0.708	4.788	756	0.7527	0.7592
0.717*	5.610	333	0.7552	0.7580
0.780	4.348	832	0.7526	0.7593
0.810*	4.966	376	0.7555	0.7585

*The experiments were performed with the connecting tube with r = 0.5353 cm.

Table (4.6)

Two Bulb Apparatus Results for the Concentration Dependence of the Diffusion Coefficient for the system He/O_2 at 300K

x_2	P (atm)	$(Pr)^{-1}$ $(atm.cm)^{-1}$	(PD_{12}) $(atm.cm^2.s^{-1})$	$(P\mathcal{D}_{12})$ $(atm.cm^2.s^{-1})$
0.064*	4.306	434	0.7455	0.7529
0.124	3.478	1041	0.7393	0.7556
0.171*	4.860	384	0.7516	0.7572
0.183	8.434	429	0.7491	0.7553
0.222	3.867	936	0.7443	0.7571
0.240	4.011	902	0.7451	0.7572
0.281*	5.604	333	0.7555	0.7598
0.346	4.659	777	0.7511	0.7604
0.373*	6.426	291	0.7580	0.7614
0.466	5.705	634	0.7551	0.7618
0.543	6.302	574	0.7590	0.7647
0.570*	7.059	265	0.7619	0.7645
0.632*	6.367	293	0.7631	0.7658
0.649	5.273	686	0.7600	0.7662
0.709*	5.678	329	0.7636	0.7664
0.784	4.365	829	0.7616	0.7684
0.788*	5.107	366	0.7639	0.7669
0.915	3.740	968	0.7616	0.7688

*The experiments were performed with the connecting tube with r = 0.5353 cm.

the experimental results.

Equation (1.18) predicts deviations from linearity at higher values of $(Pr)^{-1}$ (see fig. (1.1)), but results obtained in this work do not lie in this region.

Van Heijningen et al.[2] studied the ten noble gas binary mixtures as a function of composition and temperature, using a two bulb apparatus.

This cell was constructed so that fine precision bore capillaries could be incorporated and, hence, large values of $(Pr)^{-1}$ were encountered. Two important points appear to have been overlooked in this work:

(i) The mean free path of the gas molecules depends upon the mixture composition.[20] This may account for the concentration dependence of some gas systems that they studied being much greater than the predictions of the Chapman-Enskog theory.

(ii) The results they obtained were fitted to eqn. (1.11) by the method of least-squares. For systems containing helium, deviations of such a plot from linearity appear to be important. Experimental data in the region of curvature are included in their analysis.

The results of Van Heijningen et al.[2] offer a further test of the exactness of eqn. (1.18). More detailed knowledge of their experimental results is necessary to perform any quantitative calculations.

Table (4.7)

Shearing Cell Results for the Concentration Dependence of the Diffusion Coefficient for the system He/Ar at 300K

x_2	P (atm.)	$(P\mathcal{D}_{12})$ $(atm.cm.^2s^{-1})$
0.063	0.7450	0.7383
0.125	0.7450	0.7421
0.250	0.7450	0.7459
0.500	0.7447	0.7512
0.500	0.7447	0.7517
0.750	0.7451	0.7565
0.875	0.7452	0.7570
0.938	0.7453	0.7579

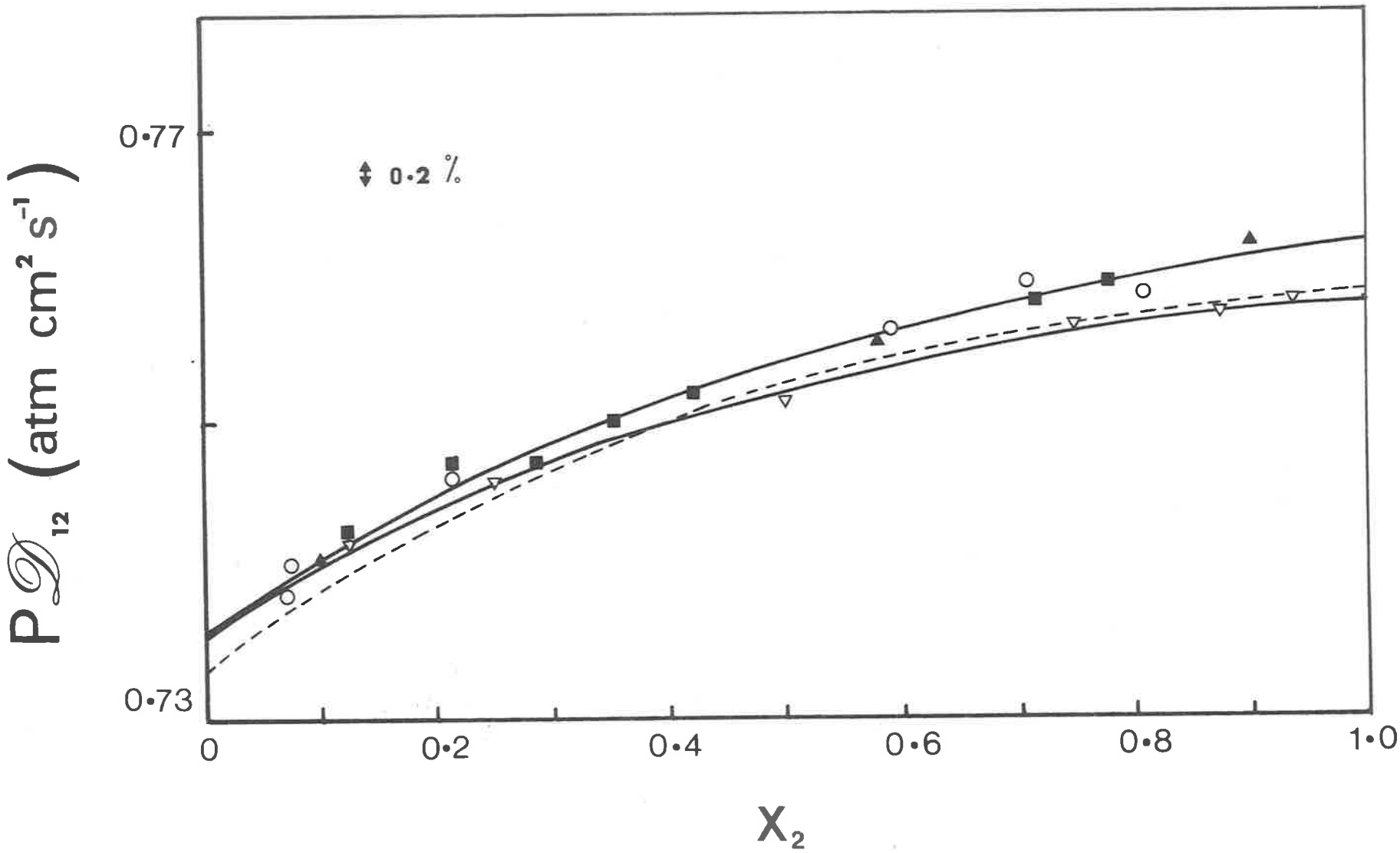

Fig. 4.4 Concentration Dependence of the Diffusion Coefficient for the system He/Ar at 300K.

■ - r = 0.5353 cm. ○ - r = 0.2763 cm. ▽ - Shearing Cell

▲ - Table 4.4 ---- Chapman-Enskog Theory

Table (4.8)

Shearing Cell Results for the Concentration Dependence of the Diffusion Coefficient for the system He/O_2 at 300K

x_2	P (atm.)	$(P\mathcal{D}_{12})$ $(atm.cm^2.s^{-1})$
0.030	0.7449	0.7478
0.063	0.7448	0.7490
0.063	0.7452	0.7498
0.125	0.7447	0.7517
0.125	0.7452	0.7519
0.250	0.7447	0.7551
0.250	0.7451	0.7553
0.500	0.7448	0.7597
0.500	0.7447	0.7604
0.500	0.7447	0.7604
0.500	0.7451	0.7608
0.750	0.7450	0.7637
0.750	0.7451	0.7639
0.875	0.7451	0.7656
0.938	0.7452	0.7665

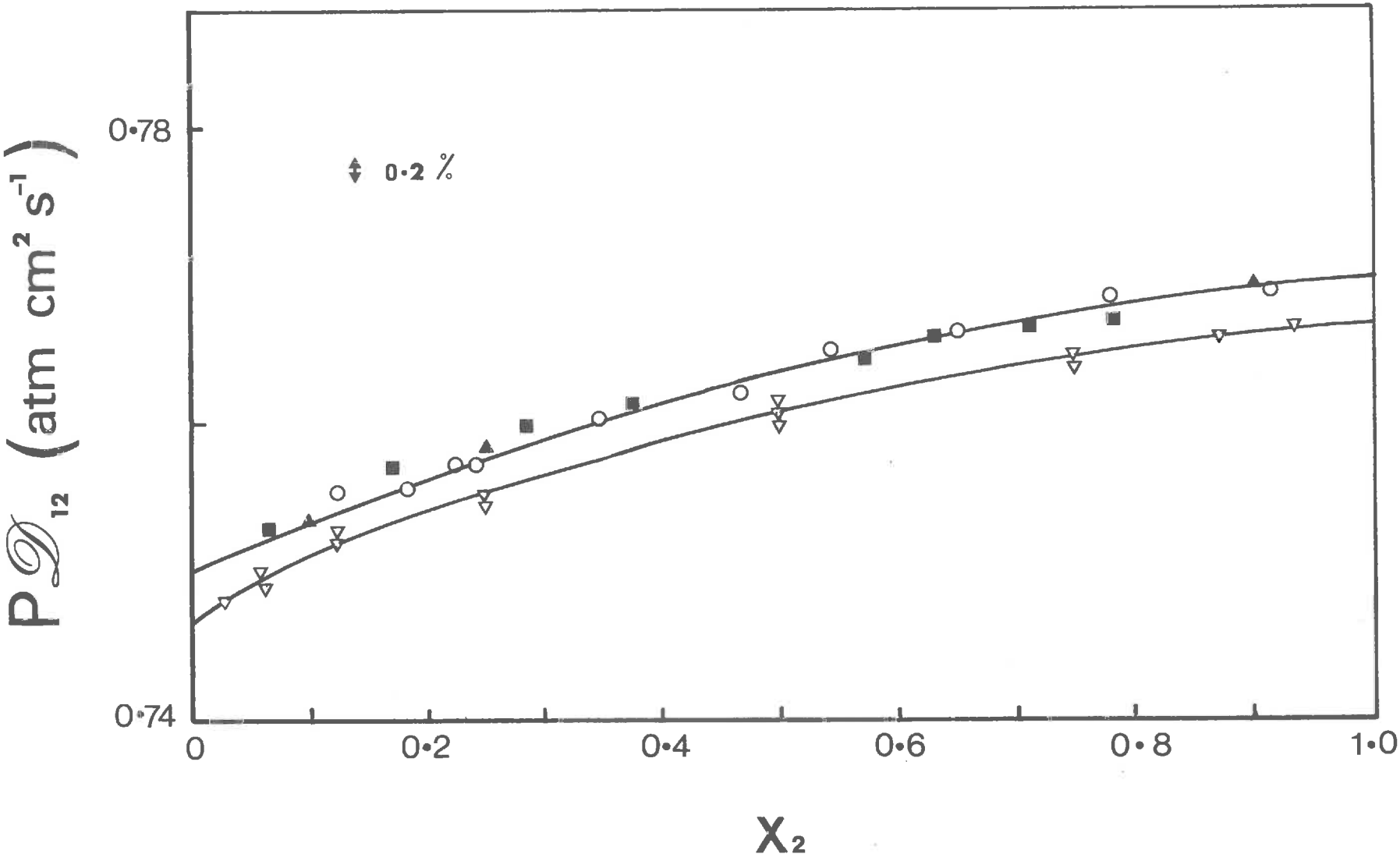

Fig. 4.5 Concentration Dependence of the Diffusion Coefficient for the system He/O_2 at 300K.

■ - r = 0.5353 cm. ○ - r = 0.2763 cm. ▽ - Shearing Cell

▲ - Table 4.4

4.3 Shearing Cell Results

Unlike the two bulb apparatus, which requires an extrapolation to determine $P\mathcal{D}_{12}$, the shearing cell gives a direct measurement of this quantity. The concentration dependences at 300K for the systems He/Ar and He/O_2, utilizing this cell are presented in Tables (4.7) and (4.8).

At these pressures of measurement the non-ideality effects discussed in Sectn.(2.14) did not appear to significantly influence the diffusion rate.

4.4 Chapman-Enskog Theory

Concentration Dependence

The concentration dependences of the two systems, using the two cells described, are presented graphically in figs. (4.4) and (4.5).

It has been shown [53,54] that the Kihara second approximation to the Chapman-Enskog theory (eqn. (1.5)) reduces to the simplified equation:

$$(P\mathcal{D}_{12}) = (P\mathcal{D}_{12})_{x_2=0}\left[1 + \frac{a_1 x_2}{1+a_2 x_2}\right] \qquad (4.1)$$

where a_1 and a_2 are constants.

This functional form provides a convenient method of summarizing concentration dependence data. Parameters, obtained from a "least-squares" analysis, are presented in Table (4.9) following.

Table 4.9

Least-square parameters of eqn. (4.1) for the systems He/Ar and He/O_2

	He/Ar			He/O_2		
	$(P\mathcal{D}_{12})_{x_2=0}$	a_1	a_2	$(P\mathcal{D}_{12})_{x_2=0}$	a_1	a_2
T.B.A.	0.7356	0.0756	1.060	0.7506	0.0506	0.947
Shearing	0.7355	0.0762	1.434	0.7469	0.0564	1.127

Kihara's second approximation to the Chapman-Enskog theory is given by eqn. (1.5). Using quantum collision integrals[17] for the Lennard-Jones potential, the concentration dependence for the two systems is predicted. Potential parameters for the He/Ar system are those derived by Van Heijningen et al.[2] The parameters for the He/O_2 system are less reliable being obtained from the combination rules.[55]

Attempting to derive parameters from the actual concentration dependence[8] yields results with large errors and, consequently, this method was not employed.

Predicted results for both systems are given in Table (4.10) following:

Table (4.10)

Predicted Diffusion Coefficients for the systems He/Ar and He/O_2 at 300K using Kihara's second approximation

x_2	He/Ar $(P\mathcal{D}_{12})_{pred.}$	He/O_2 $(P\mathcal{D}_{12})_{pred.}$
0	0.7326	0.7576
0.1	0.7384	0.7629
0.2	0.7431	0.7674
0.3	0.7469	0.7712
0.4	0.7499	0.7744
0.5	0.7522	0.7770
0.6	0.7540	0.7791
0.7	0.7555	0.7807
0.8	0.7566	0.7820
0.9	0.7575	0.7830
1.0	0.7582	0.7838

The results of Table (4.10) for the He/Ar system are shown as a dashed line in fig. (4.4). As can be seen, the agreement with the experimental results is exceptional considering the parameters are from an independent source.

The parameters for the He/O_2 system do not reproduce the data. This non-reproducibility is probably

a combination of two effects:

(i) The inability of combination rules to successfully predict mixed parameters.[2]

(ii) Failure of the Lennard-Jones potential to fit results for a diatomic molecule.

A convenient method of comparing results of the concentration dependence is to determine the ratio $\left[(P\mathcal{D}_{12})_{x_2=1} / (P\mathcal{D}_{12})_{x_2=0}\right]$ Results for both systems and those predicted by theory are given in Table (4.11).

Table (4.11)

Comparison of Experimental and Predicted Values of $(P\mathcal{D}_{12})_{x_2=1} / (P\mathcal{D}_{12})_{x_2=0}$

System	T.B.A.	Shearing	Predicted
He/Ar	1.037 ±0.005	1.031 ±0.005	1.035
He/O_2	1.026 ±0.004	1.027 ±0.002	1.035

Error limits were obtained using the 95% confidence interval.

Experimental ratios are derived from the coefficients in Table (4.10)

The error in the relaxation time measurements of the two bulb apparatus has been shown to be ±0.2%.

Taking this into account, and also as much as 0.2% experimental error in both types of cell, it may be concluded that both sets of data are in agreement.

Comparison with other Workers

Comparison with individual workers is difficult because most available data are accurate to only 1 - 2% and generally measured at different temperatures.

In recent years several correlations of diffusion data have been compiled and functions predicting diffusion coefficients over wide ranges of temperatures postulated.

These correlation functions[54,56,57] offer a convenient means of comparison. Predicted diffusion coefficients at 300K derived from these functions, as well as the experimental quantities, are presented in Table (4.12).

Table (4.12)

Comparison of Experimental Results with three Correlation Functions

	He/Ar			He/O_2		
	Exptl.	Calc.	Δ%	Exptl.	Calc.	Δ%
Ref (54) x_2=0.5	0.754	0.756	0.3	0.763	0.752	-1.5
Ref (57) x_2=0	0.736	0.726[a]	-1.3	-	-	-
Ref (56) x_2=0	0.736	0.746[a]	1.4	-	-	-

[a] Data corrected for quantum effects

The experimental values are those of the two bulb apparatus.

These correlations predict the diffusion coefficients for the He/Ar and He/O_2 system to within 2%, which is within the error of most diffusion measurements.

From this it may be concluded that these results lie within the general scatter of the literature values.

4.5 Conclusion

Binary diffusion coefficients, obtained with two cells of completely different design, have been presented. The concentration dependence of these systems has been measured and the results obtained from the two cells have been shown to agree.

Results have been given that show that the concentration differences are followed exactly and hence the correct diffusion coefficient is being measured.

An equation describing the behaviour of a binary gas mixture in capillaries at low pressures has been presented. This equation adequately describes the results in this work and also gives some insight into anomalies observed in the literature.

One may conclude that, given a carefully designed diffusion cell incorporating thermistors as the concentration measuring device, it should be possible to accurately measure binary diffusion coefficients of gases.

CHAPTER V

EFFECT OF A MAGNETIC FIELD UPON DIFFUSION

5.1 Introduction

Two previous investigations[13,14] of the effect of a magnetic field upon diffusion have revealed no significant change in this transport process. In view of the success achieved in measuring binary diffusion coefficients with thermistors as the concentration detectors, it was thought worthwhile to attempt to find such an effect. The two bulb apparatus described in Chapter II is utilized, the only alteration being a redesign of the connecting tube.

5.2 Background

Senftleben[58] first observed a change in the thermal conductivity of oxygen and nitrogen oxide under the influence of a magnetic field in 1930. A qualitative explanation of the effect, employing mean free path arguments, was given by Gorter[59,60] and later extended by Van Lier and Zernike.[61]

Little interest was shown in the subject during the subsequent 20 years until the early 1960's when two developments led to renewed interest in the topic. These were:

(i) Beenakker et al.[62] measured a field effect for nitrogen showing that the effect was

not confined to paramagnetic molecules.

(ii) Kagan and Afanas'ev[63] showed that a gradient in a gas produced a non-equilibrium distribution function which was anisotropic, not only with respect to the molecular velocities, but also with respect to the rotational angular momentum.

Kagan and Maksimov[64] recognised that it was this anisotropy that accounted for the field effects.

Boltzmann's equation is strictly applicable to monatomic gases. Since the gases that show field effects are polyatomic, the application of this equation is limited.

Problems associated with polyatomic molecules include the non-spherical symmetry of the intermolecular potential function and the internal degrees of freedom with which energy is associated. Early workers modified the theory for monatomic molecules to contain these phenomena.

In the 1940's De Boer, Wang Chang and Uhlenbeck independently presented an improved equation for polyatomic molecules. This approach[65] although not rigorous, did provide direction for later, more complete, treatments of the problem.

The rigorous theory was given by Snider,[66] and later employed by Snider and McCourt.[67,68] Continual progress in the development of the theory to include magnetic field effects is being made.

5.3 *Senftleben-Beenakker Effects*

The magnetic field effects, or "Senftleben-Beenakker" effects, are interpreted in the following manner:

Paramagnetic molecules possess a net magnetic moment so that an externally applied magnetic field will cause a precession of the magnetic moment about the direction of the field. This precession partially destroys the preferential alignments established by the gradients and collisional coupling. The magnitude of the transport coefficient will thus be altered by the presence of the field.

In the case of non-paramagnetic molecules, a small non-zero magnetic moment exists, caused by the rotational motion of the molecules and is given by:

$$\mu_{rot} = g_{rot} \mu_N J \qquad (5.1)$$

g_{rot} being the rotational Landé g-factor, μ_N the nuclear magneton and J the rotational angular momentum.

Even though the magnetic moment of non-paramagnetic molecules is considerably smaller than that for paramagnetic molecules, the field effect will be of the same magnitude since the magnetic moment acts only as a means by which precession may occur.

The value of μ_{rot} has nothing to do with the magnitude of the effect at saturation. In the case of non-paramagnetic molecules, to achieve saturation stronger magnetic field strengths must be employed to effect the same destruction of the anisotropy.

The frequency of precession is given by:

$$\omega = (2\pi\gamma\mu_0/h)H \qquad (5.2)$$

γ being the gyromagnetic ratio, μ_0 the Bohr magneton, h Plank's constant and H the magnetic field strength.

The effect must depend upon the frequency of precession, ω, as well as the average time between collisions, t_{coll}. If the product, $\omega t_{coll} << 1$ the precession is unimportant, while if $\omega t_{coll} >> 1$ the molecule will precess many times between collisions and it follows that complete averaging of orientations will result. Since t_{coll} is inversely proportional to the pressure, then ωt_{coll} is proportional to the ratio of the magnetic field strength, H, to the pressure.

Most work reported on the Senftleben-Beenakker effects show a dependence upon H/P with saturation occuring at high values of H/P.

A precessing molecule is likely to present a larger cross-sectional area than a molecule in the field free situation. This would manifest itself as an increase in the collision integral and, therefore, a decrease in the transport process would be expected.

A review article by McCourt and Beenakker[69] summarizes the methods of measurement and the results obtained for the magnetic field effect upon the thermal conductivity and viscosity of polyatomic gases. In the case of oxygen gas, each of these transport processes is decreased in magnitude by the order of 1% at saturation.

For oxygen systems, saturation occurs at H/P values as low as 50 gauss/torr.

Senftleben et al.[70] studied the thermal conduct-

ivity change in a series of binary gas mixtures involving oxygen. These results indicate that the effect decreases in the presence of another gas. In mixtures where molecular weight differences were large, the field effect was the least, while mixtures of gases with similar molecular weights to oxygen exhibited a field effect only slightly less than that of the single gas oxygen.

Heemskerk et al.[71] verified these findings. They also studied the field effect upon the concentration dependence for nitrogen-inert gas mixtures. These results indicate the preferential use of gases of similar molecular weights in attempting to find a field effect in diffusing gases.

5.4 Previous Investigations

Senftleben[13] studied the magnetic field effect in the ternery system O_2-N_2-H_2. The apparatus used consisted of two large reservoirs, each having a volume of 3000 cm^3, and connected by a system of three capillaries, the central one being so positioned that an external magnetic field could be applied.

Hot wires, positioned in the capillaries on either side of the central capillary monitored the concentration changes. These hot wires formed two arms of a Wheatstone bridge, which also included a variable resistance box for the purpose of nulling the voltage across the bridge.

In one bulb, nitrogen at a partial pressure of 20 torr was admitted, while the same partial pressure of hydrogen was introduced into the other bulb. Experiments commenced with the opening of the taps connecting the two bulbs to the capillary system. The apparatus design was

such that a large relaxation time existed and in a short period of time concentration changes would, consequently, be small. A galvanometer positioned across the Wheatstone bridge recorded deflections due to changes in gas concentrations.

Senftleben et al. assumed that the concentration varied linearly over the duration of measurements. A shift in the recorder trace occurred when a field was applied but the original trace was re-established on removing the field.

A fine wire was positioned within the central capillary in such a way that it could be moved up and down with the aid of a small electromagnet. In this manner, the cross-sectional area of the central capillary could be altered, depending upon the length of wire protruding into the capillary.

Senftleben et al. demonstrated that the relative change in cross-sectional area of the central capillary was directly proportional to the change in diffusion coefficient brought about by the applied magnetic field.

Tip et al.[72] proposed that in the experimental conditions used by Senftleben et al., the paramagnetic component would be in the equilibrium distribution and, therefore, no angular momentum anisotropy would be left to be averaged by the magnetic field. It was assumed that the effect was directly proportional to the paramagnetic component.

From the results of Senftleben et al., a change in the diffusion coefficient of 12×10^{-4} was predicted and experiments performed by Vugts et al.[14] attempted to verify these predictions.

The apparatus used in the investigation of Vugts et al. consisted of two large bulbs, each having a volume of 2000 cm^3, which were connected by a diffusion bridge. The diffusion bridge consisted of two diffusion resistances separated by a small reservoir having a volume of 2 cm^3 and constructed in such a way that a transverse magnetic field could be applied.

Using this symmetrical design, the concentration of gas in the small reservoir remains constant at all times. However, when an external magnetic field was applied to one half of the diffusion bridge, a change in the concentration of gas in the small reservoir should result. From this concentration change, measured with a mass spectrometer, the field effect upon the diffusion coefficient may be calculated. However, from these results no effect was found.

5.5 Present Investigation

The two bulb apparatus, described in section (2.2), may be utilized to measure the "Senftleben-Beenakker" effect in a diffusing gas.

A new connecting tube was used, designed so that the majority of the diffusion took place in a restriction at the centre of the tube. This enabled a solenoid to be positioned about the tube.

The solenoid consisted of coiled copper wire contained in a polyurethane casing. External connections to a second water bath, which was fitted with a water pump, provided temperature controlled, circulating water to the coils. A refrigeration unit maintained the second water

bath at a constant temperature.

Electric current to the solenoid was provided by a d.c. power supply with a maximum operating output of 60 volts. A uniform longitudinal magnetic field of up to 2000 gauss was able to be achieved. A Bell Model 640 gaussmeter (Columbus, Ohio) was used to determine the field strength at a given input voltage.

Since the partial pressure of oxygen in the experiments never exceeded 5 torr, the field strength obtained by this solenoid should have been sufficient to effect saturation.

5.6 Method of Measurement

A relative method of measurement had to be employed since the effect appears to be somewhat smaller than 12×10^{-4}. Individual experiments using the two bulb apparatus were usually only reproducible to ± 0.2%. (section (2.10))

Diffusion experiments were performed in the same manner as described in section (2.7). That is, a small quantity of gas was admitted to the cell which contained the first gas. Output voltage measurements were recorded as in a normal diffusion experiment. (section (3.2))

The relative method employed is as follows: (Reference to fig. (5.1) will be helpful at this stage.)

The experiment is commenced and data points recorded at regular intervals for a time of approximate duration, $\tau/5$, which is referred to as segment 1 in fig. (5.1). (τ is the relaxation time) This time interval is denoted Δt_1. These initial data points

establish the rate of change of concentration.

The magnetic field is applied for a period of time, Δt_2, which is designated as segment 2 in the diagram. During this interval a new diffusion rate is established, assuming the magnetic field does alter this transport process.

Finally, the magnetic field is removed and data points are recorded for the remainder of the experiment. The original diffusion rate should be re-established. This part of the experiment is referred to as segment 3 in the diagram.

The following equations describe the diffusion process in segments 1, 2 and 3. The concentration difference at the beginning of segment 3 may be given by:

$$\Delta C_3 = \Delta C_2 \exp\left[-(D_{12})_{S2}\Delta t_2/\tau'\right] \qquad (5.3)$$

where τ' is defined as (τ/D_{12}) and $(D_{12})_{S2}$ is the diffusion coefficient prevailing in segment 2. This equation may be expanded to give:

$$\Delta C_3 = \Delta C_1 \exp\left[-(D_{12})_{S1}\Delta t_1/\tau'\right] \exp\left[-(D_{12})_{S2}\Delta t_2/\tau'\right] \qquad (5.4)$$

$(D_{12})_{S1}$ being the diffusion coefficient in segment 1.

This implies that the concentration difference between the two bulbs at the commencement of segment 3 depends upon the diffusion rates established during segments 1 and 2.

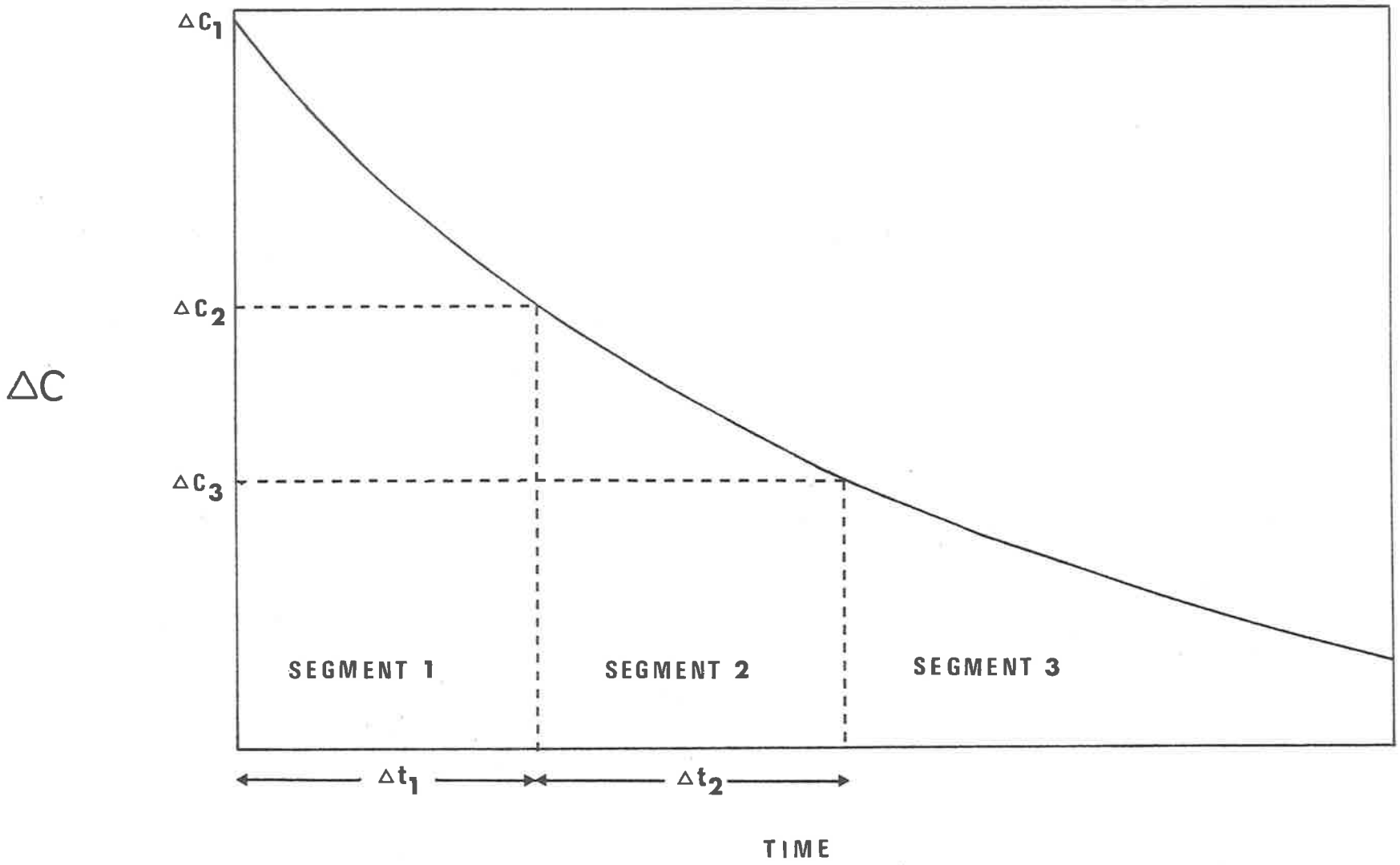

Fig. 5.1 Concentration as a Function of Time showing Division into Segments.

Equation (5.4) is equivalent to:

$$\Delta C_3 = \Delta C_1 \exp\left[(-D_{12})_{S1}(\Delta t_1 + \Delta t_2 + \delta t)/\tau'\right] \tag{5.5}$$

Equation (5.5) assumes the original diffusion rate prevails even when the magnetic field is on. The time, δt, is the interval required to account for an increase or decrease of the diffusion rate during segment 2, since a different diffusion rate will alter the concentration difference at a given point in time. This time interval is sufficient to adjust the concentration difference to ΔC_3.

Combining eqns. (5.4) and (5.5) yields:

$$((D_{12})_{S2}\Delta t_2 + (D_{12})_{S1}\Delta t_1) = (D_{12})_{S1}(\Delta t_1 + \Delta t_2 + \delta t) \tag{5.6}$$

Therefore:

$$\left[\frac{(D_{12})_{S2} - (D_{12})_{S1}}{(D_{12})_{S1}}\right] = \frac{\delta t}{\Delta t_2}$$

Thus the time increment δt divided by Δt_2 becomes a measure of the Senftleben-Beenakker effect in diffusion.

Unfortunately, the magnetic field affects the thermal conductivity of the gas about the two thermistor positions making it impossible to use data collected in segment 2. In the presence of non-paramagnetic gases no such effect is detectable. Measurement of the Wheatstone bridge voltages for a stationary oxygen environment show the effect upon the thermal conductivity to be quite reproducible and that there is no drift in these voltages

with time.

To determine the magnitude of the Senftleben-Beenakker effect in diffusion, the time interval, δt, must be determined. Data collected in segments 1 and 3 are combined and fitted to eqn. (3.5) by the method of least-squares.[38]

At the juncture between the two segments, a time interval of duration Δt_2 is substituted. By omitting successive data points, each time fitting to eqn. (3.5), any changes during the experiment in the parameters $\Delta R(\infty)$ and the relaxation time may be studied. In principle these parameters should be the same in both segments, but if the diffusion rate differs while the magnetic field is applied, then a discrepancy would be expected. By choosing an appropriate time interval, δt, the parameters in each segment may be brought into agreement.

This approach alleviates the problem of exact pressure measurement, which would be the major source of error if individual experiments are compared. The only errors of consequence in the analysis method described are the accuracy of the timing device and the standard deviation of the "least-squares fit".

The Crystal timers used produced pulses at regular time intervals, which were reproducible to 0.001%. Consequently, the error in the analysis is that due to the least-squares procedure.

Analogous arguments are valid for the situation of field on in segment 1 and off in segment 2.

5.7 *Results*

Analysis of the experimental results reduces to a study of the least-squared data. Presented in Table (5.1) are the results for the system Ar/O_2. The parameters and associated errors of the least-squares analysis are given for varying numbers of data points omitted from the beginning of the experiment. In this table, N refers to the number of data points omitted, $\Delta R(\infty)$ is the quantity defined in eqn. (3.5), (PD_{12}) the diffusion coefficient, and the columns headed "error" are the 95% confidence limits.

The number of data points "least-squared" was usually in the order of two hundred. As would be expected, errors associated with the least-squares analysis increases as the total number of data points processed, decreases.

Three different types of experiments are presented. The first type is a test experiment where data points are not recorded in segment 2 and no magnetic field is applied. This experiment will give some indication on how well segments 1 and 3 should agree when no field influence is present. The second series of experiments is when the field is applied during segment 2. The final series is the reversed situation where the field is on during segments 1 and 3.

Consider experiments 1 to 4 which are of the first type given above. All four experiments show a tendency for the calculated $\Delta R(\infty)$ value to increase and the diffusion coefficient to decrease in segment 1. After the time interval, Δt_2, (segment 2), the parameters appear

Table (5.1)

Results for the effect of a Magnetic Field upon Binary Diffusion for the System Ar/O_2

N	$\Delta R(\infty)$	Error($\times 10^3$)	$^{\dagger}PD_{12}$	Error($\times 10^5$)
		EXPT 1		
0	35.329	9.6	0.16336	6.4
3	35.331	10.0	0.16334	6.8
6	35.332	10.2	0.16332	7.4
9	35.333	10.8	0.16332	8.2
12	35.334	11.4	0.16331	9.0
15	35.337	12.0	0.16327	10.2
		Δt_2 = 8 mins.		
18	35.338	13.6	0.16326	12.6
		EXPT 2		
0	38.867	4.0	0.15007	2.6
3	38.870	3.8	0.15004	2.6
6	38.873	3.8	0.15002	2.6
9	38.875	3.8	0.15000	2.8
12	38.875	4.2	0.15000	3.2
		Δt_2 = 10 mins.		
15	38.879	4.6	0.14996	3.8
18	38.879	4.8	0.14995	4.0
21	38.879	5.0	0.14996	4.4
24	38.879	5.2	0.14996	4.6

Table (5.1) (Continued)

N	$\Delta R(\infty)$	Error($\times 10^3$)	$PD_{12}^{\dagger}$	Error($\times 10^5$)
		EXPT 3		
0	44.519	5.0	0.16440	2.8
5	44.524	4.6	0.16435	2.8
10	44.530	4.2	0.16430	2.8
15	44.536	4.4	0.16424	3.2
		Δt_2 = 8 mins.		
20	44.541	4.6	0.16419	3.8
25	44.540	5.0	0.16420	4.2
30	44.542	5.4	0.16418	4.6
		EXPT 4		
0	33.315	4.8	0.17092	3.4
3	33.319	4.8	0.17088	3.4
6	33.322	4.8	0.17086	3.4
9	33.325	4.8	0.17082	3.6
12	33.327	5.0	0.17079	4.0
		Δt_2 = 10 mins.		
15	33.332	5.6	0.17074	4.8
18	33.334	5.6	0.17072	5.0
21	33.336	5.8	0.17069	5.2
24	33.337	6.0	0.17069	5.6

Table (5.1) (Continued)

N	$\Delta R(\infty)$	Error($\times 10^3$)	$PD_{12}^{\dagger}$	Error($\times 10^5$)
		EXPT 5		
0	36.313	3.6	0.20098	3.2
3	36.315	3.4	0.20095	3.2
6	36.316	3.6	0.20094	3.4
9	36.316	3.8	0.20093	3.8
12	36.317	4.0	0.20092	4.4
		Δt_2 = 10 mins.		
15	36.316	4.6	0.20093	5.8
18	36.315	4.8	0.20095	6.2
21	36.313	5.0	0.20098	6.6
24	36.313	5.2	0.20099	7.2
27	36.312	5.4	0.20101	7.6
		EXPT 6		
0	48.042	3.2	0.19065	2.4
5	48.045	3.0	0.19061	2.6
10	48.048	3.0	0.19057	2.8
		Δt_2 = 10 mins.		
15	48.053	3.2	0.19049	3.8
20	48.053	3.4	0.19049	4.2
25	48.053	3.6	0.19048	4.8
30	48.054	3.8	0.19047	5.4

Table (5.1) (Continued)

N	$\Delta R(\infty)$	Error($\times 10^3$)	$PD_{12}^{\dagger}$	Error($\times 10^5$)
		EXPT 7		
0	42.484	5.2	0.18732	4.2
5	42.488	5.2	0.18727	4.4
10	42.491	5.4	0.18723	5.2
		Δt_2 = 10 mins.		
15	42.497	6.4	0.18714	7.0
20	42.497	6.8	0.18714	7.8
25	42.498	7.2	0.18713	8.6
30	42.501	7.6	0.18708	9.6
		EXPT 8		
0	46.315	3.4	0.20325	2.6
3	46.317	3.4	0.20322	2.6
6	46.319	3.2	0.20319	2.6
9	46.321	3.2	0.20317	2.8
12	46.322	3.4	0.20314	3.2
		Δt_2 = 10 mins.		
15	46.325	3.8	0.20312	4.0
18	46.326	3.8	0.20310	4.2
21	46.328	4.0	0.20307	4.4
24	46.328	4.0	0.20306	4.8
27	46.329	4.2	0.20306	5.6

Table (5.1) (Continued)

N	$\Delta R(\infty)$	Error($\times 10^3$)	PD_{12} †	Error($\times 10^5$)
		EXPT 9		
0	34.006	5.4	0.1882	4.0
5	34.012	5.2	0.1881	4.0
10	34.016	5.4	0.1880	6.0
		Δt_2 = 10 mins.		
15	34.019	6.4	0.1880	8.0
20	34.019	6.8	0.1880	8.0
25	34.020	7.2	0.1880	10.0
30	34.018	7.8	0.1880	10.0
		EXPT 10		
0	41.578	7.0	0.19617	6.2
3	41.581	7.0	0.19613	6.4
6	41.584	7.2	0.19610	7.0
9	41.587	7.4	0.19605	7.6
12	41.593	7.6	0.19596	8.4
		Δt_2 = 10 mins.		
15	41.608	7.4	0.19574	8.8
18	41.607	7.6	0.19576	9.2
21	41.608	7.8	0.19574	10.0

† Not necessarily the diffusion coefficient for this system.

to be more consistent. It seems that the initial data is subject to some drift, which introduces an uncertainty of approximately 0.05% in the diffusion coefficient in this segment. Parameters calculated towards the end of the segment are generally in better agreement with those of segment 3 than at the initial stages. If a longer time is waited before readings are recorded, so that the diffusing gas is given time to settle down, the rate of change of concentration would be smaller and, consequently, any effect would be more difficult to detect. It appears that these experiments are subject to some initial drift which must be considered in the analysis.

Experiments 5, 6, 7 and 8 are of the second type. The behaviour of these four experiments is similar to that of the first four, namely an initial drift of parameters in segment 1 and self-consistency of the parameters in segment 3. Parameters in segment 1 generally agree with those of segment 3 within the given confidence limits.

Experiments 9 and 10 are performed in the reverse manner to the four experiments just discussed. It might be expected that a different trend would be observed, yet the results show similar characteristics to those discussed above.

All the experiments are summarized in Table (5.2).

Within the errors of measurement the least-squares parameters agree and, therefore, there can be no basis to warrant a time shift to bring the segments into coincidence. The initial drift complicates the analysis, but taking this into consideration, there does

Table (5.2)

Summary of Results presented in Table (5.1)

Expt	x_2	Field Sequence	H/P (gauss/torr)
1	0.9	-	-
2	0.9	-	-
3	0.9	-	-
4	0.25	-	-
5	0.1	off-on-off	420
6	0.9	off-on-off	430
7	0.8	off-on-off	230
8	0.8	off-on-off	610
9	0.25	on-off-on	330
10	0.9	on-off-on	420

not appear to be any change in the diffusion rate, upon application of a magnetic field, within an uncertainty of ± 0.05%.

5.8 Discussion

Results have been presented for the system Ar/O_2 showing that the magnetic field has no effect upon the diffusion process within an estimated error of 0.05%.

Recently, Eggermont et al.[73] published their findings on the effect of a magnetic field upon thermal diffusion in the N_2/Ar system. A 1% magnitude change in this quantity was observed while using a transverse magnetic field. This effect was of the same order of magnitude as that encountered in thermal conductivity measurements for this system and it also showed the usual dependence upon H/P.

Two previous attempts[72,74] to find a field effect in thermal diffusion have revealed no magnetic field dependence.

It has been suggested by Eggermont et al.[73] that these previous workers were trying to detect too small a change in thermal diffusion in their respective apparatus. The apparatus of Eggermont et al. by contrast, however, measures a transverse thermal diffusion, thereby offering greater sensitivity.

Cooper et al.[75] have extended a theory of transport processes involving polyatomic molecules beyond that derived by Matzen et al.[76] This extension includes magnetic field effects. Expressions, based upon this theory, were derived for the magnetic field effect upon diffusion and thermal diffusion, as a function of concen-

tration, for the system N_2/Kr.

In the case of thermal diffusion, this theory predicts an effect of approximately 0.7% change. Although this is not the same system as studied by Eggermont et al.[73] the results may still be compared and such calculations do give the right order of magnitude in predicting the effect upon thermal diffusion.

Theoretical calculations for the magnetic field effect upon diffusion predict a maximum change in the diffusion coefficient of 0.002%. Unlike the theory of Tip et al.,[72] who proposed a maximum effect when the field-affected component was in trace quantities, these calculations predict a maximum at $x_2 = 0.3$. The results of Eggermont et al. are in agreement with the latter calculations.

Although Senftleben et al.[13] reported an effect of 0.02% in diffusion, his results are contestable. During an experiment a shift in the galvanometer occurred upon application of a magnetic field and, subsequently, returned to the same base line once the field was removed. (A linear change in concentration was assumed.) If the magnetic field did influence the diffusion rate, then the concentration difference between the two reservoirs would alter and, therefore, a shift in the position of the baseline would be expected once the field was applied and then removed.

It is likely that Senftleben et al. observed in fact a change in the thermal conductivity of the gas about the concentration detectors.

Vugts et al.[14] observed no effect in the systems

NO/N_2 and $^{16}O_2/^{16}O\text{-}^{18}O$ within a maximum error of 0.02%. These observations are in agreement with ref. (73).

The model proposed by Cooper et al.[73] appears to be capable of predicting the right order of magnitude of change in the quantity thermal diffusion. In view of the experimental evidence presently accruing, it would seem that the effect upon diffusion, if any, is certainly smaller than 0.05%, and hence, will be a very difficult phenomenon to measure experimentally.

APPENDICES

Page

APPENDIX I

Expressions to Evaluate Kihara's Second Approximation 103

APPENDIX II

Derivation of Expression for $\Delta R(t)$ . . . 104

APPENDIX I

EXPRESSIONS TO EVALUATE KIHARA'S SECOND APPROXIMATION

Expressions for the P's and Q's defined in section (1.2) are given below. These expressions enable Kihara's second approximation to the Chapman-Enskog theory (eqn. (1.4)) to be evaluated.

$$P_1 = \frac{2M_1^2}{M_2(M_2+M_1)} \left(\frac{2M_2}{M_1+M_2}\right)^{\frac{1}{2}} \frac{\Omega_{11}^{(2,2)*}}{\Omega_{12}^{(1,1)*}} \left(\frac{\sigma_{11}}{\sigma_{12}}\right)^2$$

$$P_{12} = 15\left(\frac{M_1-M_2}{M_1+M_2}\right)^2 + \frac{8M_1M_2A_{12}^*}{(M_1+M_2)^2}$$

$$Q_1 = \frac{2}{M_2(M_1+M_2)} \left(\frac{2M_2}{M_1+M_2}\right)^{\frac{1}{2}} \frac{\Omega_{11}^{(2,2)*}}{\Omega_{12}^{(1,1)*}} \left(\frac{\sigma_{11}}{\sigma_{12}}\right)^2$$

$$\times \left(M_1^2 + 3M_2^2 + \frac{8}{5} M_1 M_2 A_{12}^*\right)$$

$$Q_{12} = 15\left(\frac{M_1-M_2}{M_1+M_2}\right)^2 + \frac{32M_1M_2A_{12}^*}{(M_1+M_2)^2} + \frac{8(M_1+M_2)}{5(M_1M_2)^{\frac{1}{2}}}$$

$$\times \frac{\Omega_{11}^{(2,2)*}}{\Omega_{12}^{(1,1)*}} \frac{\Omega_{22}^{(2,2)*}}{\Omega_{12}^{(1,1)*}} \left(\frac{\sigma_{11}}{\sigma_{12}}\right)^2 \left(\frac{\sigma_{22}}{\sigma_{12}}\right)^2$$

where the Ω's are collisional integrals and A_{12}^* is a ratio of collision integrals. Expressions for P_2 and Q_2 are found by interchange of subscripts.

Note that the expressions for the Q's change if the Chapman-Cowling expression[54] is required.

APPENDIX II

Derivation of Expression for ΔR(t)

Consider the Circuit B as described in Chapter III with reference to fig. (3.1).

The current through each arm of the bridge is given by:

$$i_1 = \frac{V_{14}}{R_3} = \frac{V_{43}}{R_2}$$

$$i_2 = \frac{V_{12}}{R_4} = \frac{V_{23}}{R_1}$$

Combining these two equations yields:

$$(R_1 - R_2) = R_3\left(\frac{V_{23}}{V_{12}} - \frac{V_{43}}{V_{14}}\right)$$

The micacard resistors were chosen so that $R_3 = R_4$. Rearranging and making use of the following relations:

$$V = V_{12} + V_{23} = V_{14} + V_{43}$$

gives the result presented as eqn. (3.4):

$$\Delta R(t) = (R_1 - R_2) = \frac{R_3 V V_{24}}{V_{14}(V_{14} - V_{24})}$$

REFERENCES

1. Van Heijningen, R.J.J., Feberwee, A., van Oosten, A., and Beenakker, J.J.M., *Physica* 32 (1966) 1649.
2. Van Heijningen, R.J.J., Harpe, J.P., and Beenakker, J.J.M., *Physica* 38 (1969) 1.
3. Carson, P.J., Dunlop, P.J., and Bell, T.N., *J. Chem. Phys.* 56 (1972) 531.
4. Carson, P.J., Yabsley, M.A., and Dunlop, P.J., *Chem. Phys. Lett.* 15 (1972) 436.
5. Carson, P.J., and Dunlop, P.J., *Chem. Phys. Lett.* 14 (1972) 377.
6. Yabsley, M.A., Carson, P.J., and Dunlop, P.J., *J. Phys. Chem.* 77 (1973) 703.
7. Yabsley, M.A., and Dunlop, P.J., *Phys. Lett.* 3 (1972) 247.
8. Staker, G.R., Yabsley, M.A., Symons, J.M., and Dunlop, P.J., *Chem. Soc. Faraday Transactions I* 70 (1974) 825.
9. Chapman, S., and Cowling, T.G., *The Mathematical Theory of Non-uniform Gases,* Cambridge University Press, 3rd Edition, New York (1970).
10. Mason, E.A., Malinauskas, A.P., and Evans, R.B., *J. Chem. Phys.* 46 (1967) 3199.
11. Ney, E.P., and Armistead, F.C., *Phys. Rev.* 71 (1947) 14.
12. Loschmidt, J., *Akad. Wiss. Wien* 61 (1870) 367.
13. Senftleben, H., and Schult, H., *Ann. Physik* 7 (1950)103.
14. Vugts, H.F., Tip, A., and Los, J., *Physica* 38 (1968) 579.
15. Mason, E.A., *J. Chem. Phys.* 27 (1957) 75.
16. Mason, E.A., *J. Chem. Phys.* 27 (1957) 782.
17. Munn, R.J., Smith, F.J., Mason, E.A., and Monchick, L., *J. Chem. Phys.* 42 (1965) 537.

18. Neufeld, P.D., Janzen, A.R., and Aziz, R.A., *J. Chem. Phys.* 57 (1972) 1100.

19. Pollard, W.G., and Present, R.D., *Phys. Rev.* 73 (1948) 762.

20. Jeans, J.H., *The Dynamical Theory of Gases*, Dover Publications, New York (1954) p. 250.

21. Loeb, L.B., *Kinetic Theory of Gases*, McGraw-Hill, New York. p.226.

22. Shankland, I.R., Thornton, S., and Dunlop, P.J., *Chem. Phys. Lett.* 26 (1974) 533.

23. Evans, R.B., Watson, G.M., and Mason, E.A., *Chem. Phys.* 35 (1961) 2076.

24. Evans, R.B., Watson, G.M., and Mason, E.A., *J. Chem. Phys.* 36 (1962) 1894.

25. Mason, E.A., Evans, R.B., and Watson, G.M., *J. Chem. Phys.* (1963) 1808.

26. Mason, E.A., and Malinauskas, A.P., *J. Chem. Phys.* 41 (1964) 3815.

27. Zhadanov, V., Kagan, Yu., and Sazykin, A., *Soviet Phys. JETP* 15 (1962) 596. *(Zh. Exsperim.i Teor. Fiz.* 42 (1962) 857).

28. Kramers, H.A., and Kistemaker, J., *Physica* 10 (1943) 699.

29. McCarty, K.P., and Mason, E.A., *Phys. Fluids* 3 (1960) 908.

30. Suetin, P.E., and Volobuev, P.V., *Soviet Phys., Tech. Phys.* 9 (1964) 859. *(Zh. Tekh. Fiz.* 34 (1964) 1107).

31. Kotousov, L.S., *Soviet Phys., Tech. Phys.* 9 (1965) 1679. *(Zh. Tekh. Fiz.* 34 (1964) 2178).

32. Volobuev, P.V., and Suetin, P.E., *Soviet Phys., Tech. Phys.* 10 (1965) 269. *(Zh. Tekh. Fiz.* 35 (1965) 336).

33. Kosov, N.D., and Kurlapov, L.I., *Soviet Phys., Tech. Phys.* 10 (1966) 1623. *(Zh. Tekh. Fiz.* 35 (1965) 2120).

34. Rayleigh, J.W.S., *The Theory of Sound II*, Dover Publications, New York, (1945) p. 203 and p. 491.

35. Stokes, R.H., *N.Z. J. Sci. Tech. B.* 27 (1945) 75.

36. King, L.V., *Phil. Mag.* 21 (1947) 3.

37. Wirz, P., *Helv. Phys. Acta* 20 (1947) 3.

38. Wolberg, J.R., *Prediction Analysis*, Van Nostrand Co. Ltd., Princeton, New Jersey.

39. Washburn, E.W., and Smith, E.R., *J. Res. Natl. Bur. Std.* 12 (1934) 305.

40. Hall, J. McG., *Report of the Gravitational Stations in the Metropolitan Area and Salisbury*, South Australian Department of Mines, Report 59/89. (1964).

41. Barnes, C., *Physics* 5 (1934) 4.

42. Mills, R., and Woolf, L.A., *The Diaphragm Cell*, Australian National University Press, Canberra, Australia. (1968).

43. Paul, R., *Phys. Fluids* 3 (1960) 905.

44. Annis, B.K., Humphreys, A.E., and Mason, E.A., *Phys. Fluids* 12 (1969) 78.

45. Ljunggren, S., *Arkiv Kemi* 24 (1965) 1.

46. Waldmann, L., *Z. Physik* 124 (1944) 175.

47. Waldmann, L., *Z. Physik* 124 (1944) 2.

48. Waldmann, L., Z. Physik 124 (1944) 30.

49. Staker, G.S., *Unpublished data.*

50. Bolis, V.W., *Electronics* 27 (1954) 178.

51. Schmauch, L.J., and Dinerstein, R.A., *Anal. Chem.* 32 (1960) 343.

52. Van Dael, W., and Cauwenbergh, W., *Physica* 40 (1968) 165.

53. Amdur, I., and Schatzki, T.F., *J. Chem. Phys.* 29 (1958) 1.

54. Marrero, T.R., and Mason, E.A., *J. Phys. Chem. Ref. Data* 1 (1972) 3.

55. Hirshfelder, J.O., Curtiss, C.F., and Bird, R.B., *Molecular Theory of Gases and Liquids*, John Wiley and Sons, New York.

56. Marrero, T.R., and Mason, E.A., *AIChE J.* 19 (1973) 498.

57. Kestin, J., Ro, S.T., and Wakeham, W., *Physica* 58 (1972) 165.

58. Senftleben , H., *Phys. Z.* 31 (1930) 822, 961.

59. Gorter, C.J., *Naturwissenschaften* 26 (1938) 140.

60. Gorter, C.J., *Ned. Tijdschr. Natuurk.* 7 (1940) 89.

61. Zernike, F., and Van Lier, C., *Physica* 6 (1939) 961.

62. Beenakker, J.J.M., Scoles, G., Knaap, H.F.P., and Jonkman, R.M., *Phys. Lett.* 2 (1962) 5.

63. Kagan, Yu.M., and Afanas'ev, A.M., *Sov. Phys. JETP* 14 (1962) 1096 *(Zh. Eksp. Teor. Fiz.* 41 (1961) 1536).

64. Kagan, Y.M., and Maksimov, L.A., *Sov. Phys. JETP* 14 (1962) 604 *(Zh. Eksp. Teor. Fiz.* 41 (1961) 842).

65. Wang Chang, C.S., Uhlenbeck, G.E., and De Boer, J., *Studies in Statistical Mechanics* 2, North Holland Publishing Company, Holland.

66. Snider, R.F., *J. Chem. Phys.* 32 (1960) 1051.

67. McCourt, F.R.W., and Snider, R.F., *J. Chem. Phys.* 41 (1964) 3185.

68. McCourt, F.R.W., and Snider, R.F., *J. Chem. Phys.* 43 (1965) 2276.

69. Beenakker, J.J.M., and McCourt, F.R., *Ann. Rev. Phys. Chem.* 21 (1970) 47.

70. Senftleben, H., and Pietzner, J., *Phys. Z.* 34 834.

71. Heemskerk, J.P.J., Bulsing, G.F., and Knaap, H.F.P., *Physica* 71 (1974) 515.

72. Tip, A., de Vries, E., and Los, J., *Physica* 32 (1966) 1429.

73. Eggermont, C.E.J., Oudeman, P., and Hermans, L.J.F., *Phys. Lett.* 50A (1974) 173.

74. Hidalgo, M.A., Saviron, J.M., and Gonzales, D., *Physica* 46 (1970) 41.

75. Cooper, E.R., Dahler, J.S., Verlin, J.D., Matzen, M.K., and Hoffmann, D.K., *J. Chem. Phys.* 59 (1973) 403.

76. Matzen, M.K., Hoffman, D.K., and Dahler, J.S., *J. Chem. Phys.* 56 (1972) 1486.